

Contents lists available at ScienceDirect

Applied Mathematical Modelling

journal homepage: www.elsevier.com/locate/apm



An eco-epidemiological model with social predation subject to a component Allee effect



Lisha Wang^{a,b}, Zhipeng Qiu^{a,*}, Tao Feng^{a,b}, Yun Kang^b

- ^a School of Science, Nanjing University of Science and Technology, Nanjing 210094, PR China
- b Science and Mathematics Faculty, College of Integrative Sciences and Arts, Arizona State University, Mesa, AZ 85212, USA

ARTICLE INFO

Article history: Received 28 May 2020 Revised 20 June 2021 Accepted 24 July 2021 Available online 20 August 2021

Keywords: Eco-epidemiological model Component Allee effect Cooperative hunting Mating limitation

ABSTRACT

Allee effect plays important roles in social species' survival, invasion and evolution. The dynamical characteristics of populations incorporating component Allee effect and infectious disease remain unclear. In this paper, we propose an eco-epidemiological model of prey and predator interactions with assumptions that (1) The predator has cooperative social behavior in hunting prey; (2) The predator experiences component Allee effect generated from limited mating; (3) The disease can spread among predators, Our proposed model is novel to study the joint effects of cooperative behavior, mating limitation and disease in predator. We first investigate the dynamics of the disease-free model in four cases based on whether predators have mate limitation or cooperation as well as oneand two-parameter bifurcations. Analytical results show that the introduction of mate limitation generates a strong Allee effect and Hopf bifurcation. It is found that increasing mate limitation in a reasonable region stabilizes the system, but excessive limiting strength would lead the coexistence equilibrium to go extinction. We also study the dynamics of the predator-prey model in presence of disease. The theoretical result shows that the model always has a predator-extinction equilibrium which is always locally stable. We then explore how mate limitation affect the transmissibility of disease among cooperative predators. The results show that mating limitation can save the predator from disease-driven extinction and lead the disease to disappear from the system when the cooperation coefficient is large, while it drives the predators to die out if the cooperation coefficient is small. Our results indicate that the proposed model incorporating component Allee effect exhibits rich and complex dynamic behaviors. The interesting findings provide more perspectives on protection and disease control of populations in complex communities.

© 2021 Elsevier Inc. All rights reserved.

1. Introduction

Infectious disease has been an enormous threat to global wildlife conservation and human health. Smith et al. [1] have shown that 4% of species extinction and 8% of the endangered status of species since 1500 are related to the spread of infectious disease. Recent study [2] has predicted that human mortality caused by infectious disease remains about 13–15 million annually until at least 2030. These evidence indicate that it is still a major challenge for human public health to control the exposure of infectious diseases in plants and animals. As we all know, disease outbreaks must take place in

E-mail addresses: lswang.math@gmail.com (L. Wang), nustqzp@njust.edu.cn (Z. Qiu), tfeng,math@gmail.com (T. Feng), yun.kang@asu.edu (Y. Kang).

^{*} Corresponding author.

ecological communities. Generally, there are many species involved in the infection dynamics of disease. In 2015, Johnson et al. [3] summarized the reasons why infectious disease research needs community ecology, and pointed out that managing the challenges of emerging infectious disease requires a clear understanding of the full ecological context of infection and transmission. Since the changes of environmental factors in the ecological community are likely to regulate or enhance the disease further transmission [4], and the prevalence of disease may also threaten the species' survival even alter entire community structure [5]. Thus, it is essential to study the interactions between ecological communities and the related infectious diseases spreading for implement management efforts.

Mathematical modeling has contributed significantly to our understanding of both the ecosystem and the epidemiology of infection diseases [6–10]. Eco-epidemiological model describes interspecific interaction between species as well as transmission dynamics of the disease, and is a powerful theoretical tool for analyzing the above eco-epidemiological issues. The use of eco-epidemiological model to study the impact of the disease on ecological community can date back to the work of Anderson and May [11]. Since then, there have been many studies focused on the predator-prey models with the disease among the prey/predator population ([12–16] and the references therein). Sasmal and Chattopadhyay [12] provided a general eco-epidemiological predator-prey model with the predators subject to weak Allee effect, and demonstrated that weak Allee effect can create or destroy the predators' survival. Kang et al. [13] considered strong Allee effect occurring in the preys, and showed that the disease can save the prey from predation-driven extinction. The two studies assume that the disease spread among the population of preys, while the infectious disease can also cause trouble in predators. Su et al. [14] explored the impacts of the disease on the predators which are subject to weak Allee effect in an eco-epidemiological model. These works provide useful insights into the ecological context of infection and transmission.

The above mentioned eco-epidemiological predator-prey models incorporate weak or strong Allee effect which are demographic Allee effects, i.e., a positive relationship between the overall individual fitness and population density (usually quantified by the per capita growth rate [17]). Besides the demographic Allee effect, a component Allee effect is also a significant subcategory of Allee effect used in the ecology literature which is the positive relationship between any measurable component of individual fitness and population size or density. Some literature has shown that various ecological mechanisms can generate component Allee effects in the natural community, including mate limitation [18], cooperative feeding [19] and cooperative breed [20]. Recently, the research by Bourbeau-Lemieux contributes to the evidence that the component Allee effects can exacerbate the effects of other environmental drivers and increase the risk of extinction of small-size populations [21]. Therefore, it is meaningful to understand a particular specie and its ecological conservation by considering the varying component fitness. Some researchers have recognized the need for the exploration of component Allee effect by using theoretical models and have achieved some good findings. Terry [22] explored four predator-prey models with a component Allee effect induced by mating limitation, and they found that the predator will always die out if the initial density of predator or prey population is sufficiently small. Aguirre et al. [23,24] investigated the Leslie-type predator-prey models with a component Allee effect induced by the reducing breeding at low densities, and gave the conditions for the long-term extinction or survival of predator and prey populations.

Group hunting behavior also widely exists in the predator-prey model as well as Allee effect mechanisms ([25–27]). Cooperative hunting is common among the animals, which benefits the survival of predators as a result of getting enough food through cooperation [28–30]. There are many living communities that search and attack preys by cooperation, such as lions [31], African wild dogs [32], wolves [33], birds [34] and ants [35]. Mathematical modelling of cooperative hunting behavior has been studied extensively. Cosner et al. [36] proposed a predator-prey model with various forms of functional response function which takes into account the spatial distribution of predators and opportunities for predation. Berec [37] formulated a generalized cooperative hunting model and showed that the cooperation can destabilize the coexistence of the model and lead to oscillations. Alves and Hilker [30] did an extended work on a predator-prey model with hunting cooperation in the predator, and explored the impact of hunting cooperation on the density of population and stability of the ecological model. Some insightful reviews pointed that the social hunting behavior and component Allee effect can co-occur in several species [17,19,38]. Therefore, it is meaningful to incorporate the hunting cooperation into a mathematical model that described a living community experienced component Allee effect. This is one of our main concerns in the paper.

Many researchers have investigated the eco-epidemiological predator-prey model with social hunting behavior (i.e., [28,39]). For instance, Hilker et al. [28] presented a predator-prey model with social predation subject to infectious disease, and the results showed that the system has bistable dynamics, i.e., the predator population with low-size goes to extinction driven by disease, while the predator population with high-size survives due to strong hunting cooperation. In reality, there is such a scenario that the population dynamics of some social species may be influenced by Allee effects and some diseases simultaneously. For instance, wolves are typical monogamous mammals preying in groups and search for mates only within a maximum distance [40–42], and various pathogens of wolf disease have been observed in the southern Lake Superior region where wolves are subject to a weak Allee effect induced by mate-finding. Inspired by the characteristics of wolves as described in the above example, in this paper, we propose a predator-prey model with the diseased predator subject to mating limitation and cooperative hunting. This theoretical framework is expected to reveal how the interplay among disease, mating limitation, and hunting cooperation can affect the dynamical pattern of the system, especially for the impact on the establishment and extinction of disease.

The rest of this paper is organized as follows: in Section 2, we present the derivation of our model and give the primary results; in Section 3, we investigate the dynamical behaviors of the disease-free model in four cases, and present bifurcation diagrams to illustrate the biological effects of mating limitation and cooperation on the dynamics of predator and prey; in

Section 4, the dynamics of the full model is analyzed, and the bifurcation diagrams are carried out to explore the joint effects of key factors including the disease transmission rate, the mating limitation parameter and the cooperation coefficient on the population dynamics; in Section 5, we end this paper with a discussion.

2. Model formulation

In this section, we formulate the eco-epidemiological model with social predation subject to mating limitation and disease.

The population of prey and predator are denoted by N and P respectively. In the absence of predation, we assume that the dynamics of the prey population is described by the logistic equation, i.e., $\frac{dN}{dt} = rN(1 - \frac{N}{K})$, where r is the intrinsic growth rate, K is the environmental carrying capacity. In the presence of predation, we assume that the predators are specialists and generally capture the preys through cooperation. The cooperative behaviour in hunting is considered to increase the successful attack rate with the increasing density of predators. Alves, Hilker et al. [28–30] propose a density-dependent function $\phi(P) = a + bP$ to model the attack rate, where $a \ge 0$ is the constant attack rate of individual predator without cooperation, $b \ge 0$ is the strength of cooperation. In this paper, we also choose the above function to describe the cooperative hunting behaviour of the predator. This gives

$$\frac{dN}{dt} = rN\left(1 - \frac{N}{K}\right) - (a + \underbrace{bP}_{\text{Effects of cooperation in hunting}})NP,$$

$$\frac{dP}{dt} = e(a + bP)NP - mP,$$
(1)

where m is the natural death rate of the predator. In the case that there is no cooperation in hunting, we have b = 0 and the model (1) reduces to the traditional Lotka–Volterra model

$$\frac{dN}{dt} = rN\left(1 - \frac{N}{K}\right) - aNP,$$

$$\frac{dP}{dt} = eaNP - mP.$$
(2)

Now we consider predator experiences mating limitation that affects its own reproduction. We assume that the reproduction of predator is affected by mating limitation that can be modeled by $\frac{P}{P+\alpha}$ based on the biological support [43]. We ignore the time delay due to gestation, and assume that the growth rate of predator is proportional to the product of the predation rate and a component Allee effect due to mating limitation, i.e., $e^{\frac{P}{\alpha+P}}(a+bP)NP$, where $0 < e \le 1$ is the efficiency of energy conversion. Based on the above assumptions, the predator-prey model with predator subject to component Allee effect and hunting cooperation can be described by the following ODE equations:

$$\frac{dN}{dt} = rN\left(1 - \frac{N}{K}\right) - (a + bP)NP,
\frac{dP}{dt} = e \quad \underbrace{\frac{P}{\alpha + P}} \quad (a + bP)NP - mP.$$
(3)

In the presence of infectious disease in predator, we assume that there is only one disease which spreads among predators, and the total predators P are divided into two subclasses: susceptible and infectious which are denoted by S and I respectively. The susceptible predators are assumed to acquire infection of the disease at the rate βSI , where β is the transmission rate of disease. In addition, we also assume that: (a) the infected predator will transmit the infectious disease vertically; (b) the infected predator can not recover from the disease, and will lead to an additional disease-induced death rate; (c) the disease has little effect on cooperative hunting behaviour (the successful attack rate in predation) and mating rate. The assumption (c) indicates that the susceptible and infected predators have the same density-dependent cooperation strength b, and the attack rates $\phi(S,I)$ of the susceptible and infected predators are both described by the function $\phi(S,I) = a + b(S+I)$, which has been proposed in the paper [28]. The assumption (c) also indicates that the presence of disease has little effect on predators' mating, i.e., any individual in predator population has equal opportunity to mating successfully with rate $\frac{S+I}{\alpha+S+I}$. Based on the assumptions, we have the following differential equations to describe the ecoepidemiological predator-prey model with the social predator subject to component Allee effect:

$$\frac{dN}{dt} = rN\left(1 - \frac{N}{K}\right) - [a + b(S+I)]N(S+I),$$

$$\frac{dS}{dt} = e\frac{S+I}{\alpha+S+I}[a+b(S+I)]NS - \beta SI - mS,$$

$$\frac{dI}{dt} = e\frac{S+I}{\alpha+S+I}[a+b(S+I)]NI + \beta SI - mI - \mu I.$$
(4)

Table 1 Equilibria and their stability of model (3) in case (a), where $N_* = \frac{m}{ea}$, $P_* = \frac{r}{a} \left(1 - \frac{m}{eaK}\right)$.

Equilibrium	Existence	Stability Condition
$E_0(0,0)$ $E_K(K,0)$ $E_*(N_*, P_*)$	always always ^{<u>Kea</u>} > 1	always unstable globally asymptotically stable if $\frac{\mathit{Kea}}{m} < 1$ globally asymptotically stable if it exists

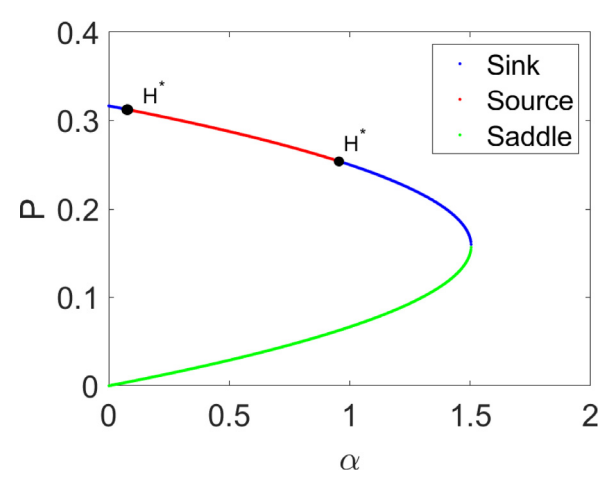


Fig. 1. One parameter bifurcation diagram describes the number of positive equilibria and their changes in stability when α increases from 0 to 2. The following parameters are used: r = 1, K = 10, e = 0.2, m = 0.3, and a = 3. In Fig. 1, the blue line represents sink, the green line represents saddle, the red line represents source, and H^* denotes Hopf bifurcation.

The purpose of this paper is to understand how the Allee parameter α and the transmission rate of disease β affect the dynamics of the predator-prey model (4). In order to carry out the investigation, we present some preliminary results first. Let

$$\Omega = \bigg\{ (N,S,I) \in \mathbb{R}^3_+ : 0 \leq N \leq K, 0 \leq N+S+I \leq \frac{M}{m} \bigg\},$$

where $M = \frac{K(r+m)^2}{4r}$. Then we have

Theorem 1. The set Ω is positive invariant, and all solutions of the model (4) are ultimately bounded within the region.

3. Dynamics of the populations without disease in predator

In order to investigate the dynamical behaviors of model (4), in this section let us first study the dynamics of model (3). Straightforward computation yields that the model (3) always has two boundary equilibria $E_0(0,0)$, $E_K(K,0)$. For convenience, when the model (3) has a unique positive equilibrium, we define it as $E_*(N_*, P_*)$; when the model (3) has two positive equilibria, we define them as $E_1^*(N_1^*, P_1^*)$, $E_2^*(N_2^*, P_2^*)$ where $P_1^* < P_2^*$. Next, based on the existence of cooperation and mating limitation, we discuss the model (3) in four cases.

Case (a): $\alpha=0$, b=0. In the absence of mating limitation and hunting cooperation, the predator-prey model (3) is the classical Lotka-Volterra predator-prey model with a logistic growth in prey population. It is well known that the dynamical behavior of the model (3) in this case is completely determined by $\frac{Kea}{m}$ which is called the basic reproduction number of predator. If $\frac{Kea}{m} < 1$, the boundary equilibrium E_K is globally asymptotically stable; if $\frac{Kea}{m} > 1$, the model has a positive equilibrium E_* which is globally asymptotically stable. All the above results can be seen in Table 1.

Case (b): $\alpha > 0$, b = 0. In the absence of hunting cooperation, the model (3) is reduced into

$$\frac{dN}{dt} = rN\left(1 - \frac{N}{K}\right) - aNP,$$

$$\frac{dP}{dt} = ea\frac{P}{\alpha + P}NP - mP.$$
(5)

The classification for the existence and local stability of the equilibria is summarized in Theorem 2. In order to illustrate the impact of α on the stability of coexistence equilibria of model (5), we also present the one-parameter bifurcation diagrams with varying α as shown in Fig. 1.

Table 2 Equilibria and their stability of model (5), where $N_{1,2}^* = K - \frac{(eaK - m) \mp \sqrt{(m - eaK)^2 - 4\frac{K}{\epsilon}ea^2m\alpha}}{2ea}$, $P_{1,2}^* = \frac{(eaK - m) \mp \sqrt{(m - eaK)^2 - 4\frac{K}{\epsilon}ea^2m\alpha}}{2eaK - 2}$.

		- cu
Equilibrium	Existence	Stability Condition
$E_0(0,0)$	always	always unstable
$E_K(K, 0)$	always	locally asymptotically stable
$E_1^*(N_1^*,P_1^*)$	$\frac{\mathit{Kea}}{\mathit{m}} > 1$ and $\alpha < \frac{(\mathit{m}-\mathit{eaK})^2\mathit{r}}{4\mathit{ea}^2\mathit{mK}}$	saddle if it exists
$E_2^*(N_2^*,P_2^*)$	$\frac{\textit{Kea}}{\textit{m}} > 1 \text{ and } \alpha < \frac{(\textit{m}-\textit{eaK})^2 \textit{r}}{4\textit{ea}^2 \textit{mK}}$	locally stable if $\frac{r}{K} > ea \frac{\alpha P_2^*}{(\alpha + P_2^*)^2}$

Table 3 Equilibria and their stability of model (1).

Equilibrium	Existence	Stability Condition
$E_0(0,0)$ $E_K(K,0)$	always always	unstable locally asymptotically stable if $\frac{\textit{Kea}}{\textit{m}} < 1$
$E_*(N_*,P_*)$	$\frac{\textit{Kea}}{m} > 1$; or $\frac{\textit{Kea}}{m} = 1$, $\frac{a^2}{r} < b$	locally asymptotically stable if $\frac{r}{K} > ebP_*$
$E_1^*(N_1^*, P_1^*)$	$\frac{Kea}{m} < 1$, $\frac{a^2}{r} < b$ and	saddle if it exists
$E_2^*(N_2^*, P_2^*)$	$\frac{m}{eK} < \frac{2\left(a^2 + 3br\right)\left[a + \sqrt{a^2 + 3br}\right] + 3br}{27br}$ $\frac{Kea}{m} < 1, \frac{a^2}{r} < b \text{ and}$ $\frac{m}{eK} < \frac{2\left(a^2 + 3br\right)\left[a + \sqrt{a^2 + 3br}\right] + 3br}{27br}$	locally asymptotically stable if $\frac{r}{R} > ebP_2^*$
	$\frac{m}{eK} < \frac{27br}$	

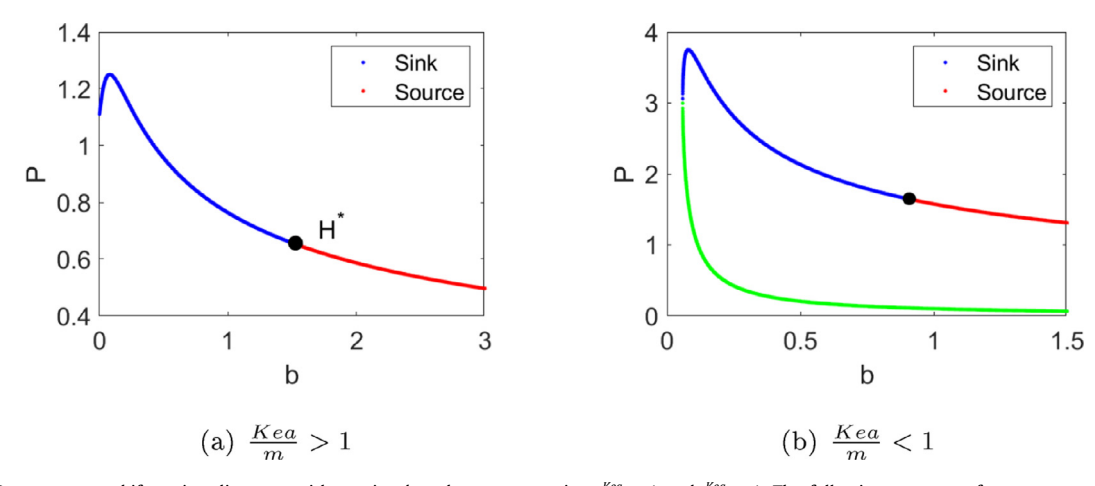


Fig. 2. One parameter bifurcation diagrams with varying b under two scenarios: $\frac{Kea}{m} > 1$ and $\frac{Kea}{m} < 1$. The following two sets of parameters are used in Fig. 2(a) and (b), respectively: (a) r = 1, K = 5, a = 0.3, e = 0.2, m = 0.2; (b) r = 3, K = 10, a = 0.1, e = 0.2, m = 0.4. Fig. 2 describes the number of positive equilibria and their changes in stability as increasing b, where the blue line represents sink, the green line represents saddle, the red line represents source, and H^* denotes Hopf bifurcation.

Theorem 2. The model (5) always has two boundary equilibria $E_0(0,0)$ and $E_K(K,0)$, and can have up to two positive equilibria. Sufficient conditions for the existence and stability of these equilibria are shown in Table 2.

According to Theorem 2, the model may have two positive equilibria E_1^* and E_2^* when α is small, where E_2^* is locally stable and E_1^* is a saddle. Under such a scenario, the model has two attractors: E_K and the coexistence attractor E_2^* , and the predator may die out or coexist with the prey depending on its initial conditions. It implies that the mating limitation parameter α can generate strong Allee effects in predator when α is not large enough. Moreover, the bifurcation diagram in Fig. 1 suggests that: (a) Large values of α can reduce the size of predator population; (b) Increasing the values of α can destabilize first and then stabilize the system, but too large values lead to the extinction of predator population and leave only prey to survive in the system.

Case (c): $\alpha = 0$, b > 0. In this case, the predator-prey model has no mating limitation in predator. The model (3) is reduced into model (1), which has been proposed in the paper [30]. In [30], the authors show that strong hunting cooperation (b > 0) can ensure the persistence of the predator population when predators would extinct in the absence of hunting cooperation by numerical simulations. In this paper, we study the dynamical behaviors of this model theoretically, and provide sufficient conditions for the existence and stability of equilibria. We summarize the results of model (1) in Theorem 3, and also

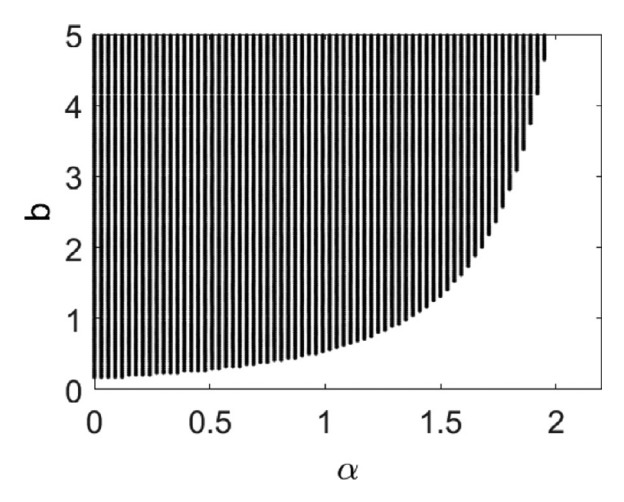


Fig. 3. Two parameter bifurcation diagrams in $\alpha - b$ plane describes the number of positive equilibrium with varying α and b, and the following parameters are used : r = 3, K = 5, a = 0.1, e = 0.2, m = 0.3. In the black region, the model (3) has two positive equilibria; in the white region, the model (3) has no positive equilibrium.

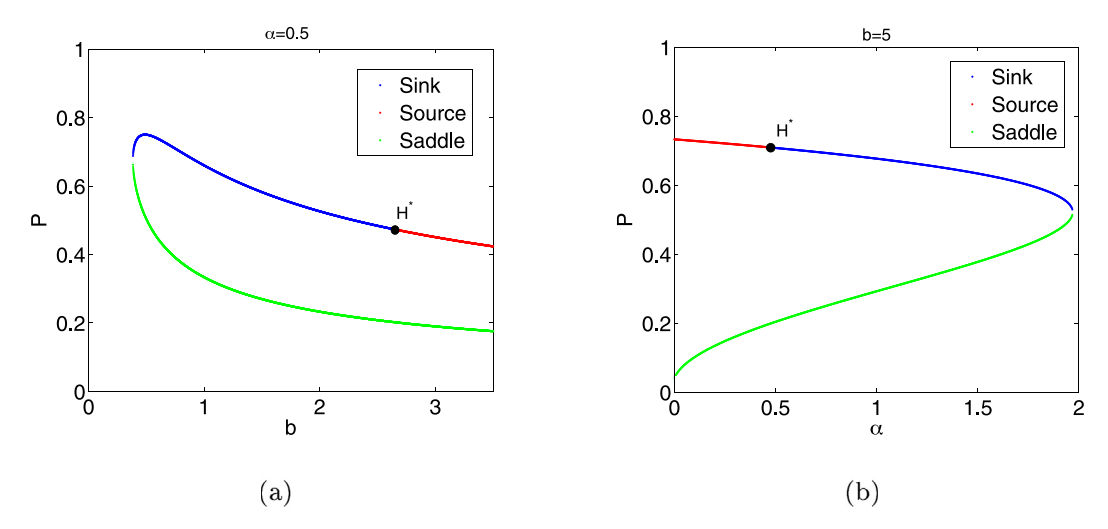


Fig. 4. One parameter bifurcation diagrams in Fig. 4 describe the stability of positive equilibrium as increasing b and α respectively. We fix r=1, K=5, a=0.3, e=0.2, m=0.2, m=0.2, m=0.3, m=0.2, m=0.3, m=0.3,

present the bifurcation diagrams with varying cooperation coefficient *b* in Fig. 2 to explore the impact of cooperation on the dynamics of predator.

Theorem 3. The model (1) always has two boundary equilibria $E_0(0,0)$ and $E_K(K,0)$, and can have up to two positive equilibria. Sufficient conditions for the existence and stability of these equilibria are shown in Table 3.

According to Theorem 3, the number of positive equilibrium can be classified into two scenarios: if $\frac{Kea}{m} > 1$, the model can have only one positive equilibrium; if $\frac{Kea}{m} < 1$, the model may have zero or two positive equilibria. It indicates that the basic reproduction number of predator $\frac{Kea}{m}$ is very important for the model (1). Under the second scenario, large b enables the model to exhibit two positive equilibrium E_1^* and E_2^* , where E_2^* may be locally stable while E_1^* is a saddle. It suggests that the model has bistability between E_K and E_2^* , and a large cooperation coefficient b can generate strong Allee effect. Moreover, the bifurcation diagrams in Fig. 2(a) and (b) correspond to above two scenarios respectively, which provide the additional information that: (a) increasing the values of b can increase first and then reduce the size of predator population; (b) too large value of b destabilizes the system and leads to a Hopf bifurcation.

Case (d): $\alpha > 0$, b > 0. In this case, the model (3) has both mating limitation and hunting cooperation in predator. The classification for the existence and local stability of the equilibria is summarized in Theorem 4. In order to explore the impacts of α and b on the existence and stability of model (3), one-parameter and two-parameter bifurcation diagrams are simulated as shown in Figs. 3 and 4.

Table 4 Equilibria and their stability of model (3) when $\alpha > 0$ and b > 0. See the Appendix D for the detailed expressions of γ_2 , η and function H(P).

Equilibrium	Existence	Stability Condition
$E_0(0,0)$ $E_K(K,0)$ $E_1^*(N_1^*, P_1^*)$	always always $\frac{e \alpha K}{m} > 1, H(\eta) < 0 \text{ or }$	always unstable locally asymptotically stable saddle if it exists
$E_2^*(N_2^*, P_2^*)$	$\begin{array}{l} \frac{e\alpha K}{m} < 1, \ b > \frac{\alpha^2}{r}, \ H'(\gamma_2) < 0, \ H(\eta) < 0 \\ \frac{e\alpha K}{m} > 1, \ H(\eta) < 0 \ \text{or} \\ \frac{e\alpha K}{m} < 1, \ b > \frac{\alpha^2}{r}, \ H'(\gamma_2) < 0, \ H(\eta) < 0 \end{array}$	locally asymptotically stable if $\frac{r}{R} > eb \frac{p_2^{*2}}{\alpha + p_2^*} + e \frac{\alpha P_2^*}{(\alpha + p_2^*)^2} (a + bP_2^*)$

Theorem 4. The model (3) always has two boundary equilibria $E_0(0,0)$ and $E_K(K,0)$, and may have zero or two positive equilibria. Sufficient conditions for the existence and stability of these equilibria are shown in Table 4.

Table 4 shows the sufficient conditions for the existence of positive equilibrium. From $H(\eta) < 0$, we can get that $\alpha < -\left(\frac{eb^2K}{mr}\eta^4 + \frac{2eab^2K}{mbr}\eta^3 + \frac{(a^2-br)eb^2K}{mb^2r}\eta^2 + \frac{m-eaK}{m}\eta\right)$. It indicates that a smaller value of α is beneficial to the existence of positive equilibrium. Similarly, $b > \frac{a^2}{r}$ implies that the model has a positive equilibrium when the value of b is large. However, due to the complexity of these conditions, the above implications are part of the information that explains the impact of α and b on the dynamical behavior of positive equilibrium. Therefore, we take bifurcation diagram in Fig. 3 to illustrate the effects of both the parameters intuitively. From Fig. 3, large values of b and small values of b favor the existence of positive equilibrium. Moreover, the one-parameter bifurcations in Fig. 4 suggest that b and a can affect the dynamics of model (3) in three ways: (a) increasing b as well as a is potential to reduce the size of predator population; (b) too large values of b destabilize the system and lead to a Hopf bifurcation; (c) large values of a are potential to stabilize the system, but too large values lead all the predator to go extinction. Fig. 4 also indicates that a and b can generate strong Allee effect since the model exhibits bistability between the boundary equilibrium a and a can affect the dynamics of the system, but too

4. Dynamics of populations with disease in predator

In this section, we consider the dynamics of full model (4).

Straight forward computation yields that the model (4) always has two boundary equilibria $E_0(0,0,0)$ and $E_K(K,0,0)$. In order to classify the existence of other equilibria of model (4), we first define two functions F(P), G(P) as

$$\begin{split} F(P) := & K - \frac{K}{r}(a + bP)P - \frac{m(\alpha + P)}{e(a + bP)P} \\ = & \frac{1}{e(a + bP)P} H(P), \\ G(P) := & K - \frac{K}{r}(a + bP)P - \frac{(m + \mu)(\alpha + P)}{e(a + bP)P}. \end{split}$$

By using the same arguments in the discussions of model (3), the positive roots of the functions F(P) and G(P) provide us the information on the number of boundary equilibria of model (4) on N-S and N-I coordinate plane respectively. For convenience, we denote the two boundary equilibrium on the N-S plane as $E_1^S(N_1^S, S_1^S, 0)$, $E_2^S(N_2^S, S_2^S, 0)$ where $S_1^S < S_2^S$, and the two boundary equilibria on the N-I plane as $E_1^I(N_1^I, 0, I_1^I)$, $E_2^I(N_2^I, 0, I_2^I)$ where $I_1^I < I_2^I$. The model (4) may have zero or two boundary equilibria on both N-S and N-I coordinate planes depending on the signs of $F(S_c)$ and $G(I_c)$, where S_c and I_c are extreme points such that $F'(S_c) = 0$, $G'(I_c) = 0$. The detailed sufficient conditions for the existence of E_1^S , E_2^S , E_1^I and E_2^I are summarized in Table 5.

Assume that $E_*(N_*, S_*, I_*)$ is the positive equilibrium of model (4). Then we have

$$r\left(1 - \frac{N_*}{K}\right) - [a + b(S_* + I_*)](S_* + I_*) = 0,$$

$$e\frac{S_* + I_*}{\alpha + S_* + I_*} [a + b(S_* + I_*)]N_* - \beta I_* - m = 0,$$

$$e\frac{S_* + I_*}{\alpha + S_* + I_*} [a + b(S_* + I_*)]N_* + \beta S_* - m - \mu = 0.$$
(6)

Subtracting the third equation from the second equation gives that $S_* + I_* = \frac{\mu}{\beta}$. Then, by substituting $S_* + I_* = \frac{\mu}{\beta}$ into the first equation, we obtain

$$N_* = K \left[1 - \frac{1}{r} (a + \frac{b\mu}{\beta}) \frac{\mu}{\beta} \right].$$

Table 5 Equilibria and their stability of model (4).

Equilibrium	Existence	Stability Condition
$E_0(0,0,0)$ $E_K(K,0,0)$	always always	unstable locally asymptotically stable
$E_1^S(N_1^S, S_1^S, 0)$ $E_2^S(N_2^S, S_2^S, 0)$	$F(S_c) > 0$ $F(S_c) > 0$	a saddle if it exists locally asymptotically stable if $\frac{\mu}{\beta} > S_2^{\rm S}$ and
$E_1^l(N_1^l, 0, l_1^l)$ $E_2^l(N_2^l, 0, l_2^l)$	$G(I_c) > 0$ $G(I_c) > 0$	$\frac{r}{R} > eb \frac{(S_2^5)^2}{\alpha^4 + S_2^5} + e \frac{\alpha S_{12}}{(\alpha + S_2^5)^2} (a + bS_2^5)$ a saddle if it exists locally asymptotically stable if $\frac{\mu}{\beta} < l_2^l$ and
$E_*(N_*,S_*,I_*)$	$F\left(\frac{\mu}{\beta}\right) > 0, G\left(\frac{\mu}{\beta}\right) < 0$	$\begin{split} &\frac{r}{K} > eb\frac{(l_2^l)^2}{\alpha + l_2^l} + e\frac{al_2^l}{(\alpha + l_2^l)^2}(a + bl_2^l) \\ &\text{locally asymptotically stable if } a_1(E_*) > 0, \\ &a_1(E_*) > 0 \text{ and } a_1(E_*)a_2(E_*) > a_0(E_*) \end{split}$

It then follows that

$$S_* = \frac{1}{\beta} \left[m + \mu - e \frac{\frac{\mu}{\beta}}{\alpha + \frac{\mu}{\beta}} (a + \frac{b\mu}{\beta}) N_* \right], \quad I_* = \frac{1}{\beta} \left[e \frac{\frac{\mu}{\beta}}{\alpha + \frac{\mu}{\beta}} (a + \frac{b\mu}{\beta}) N_* - m \right].$$

The existence of positive equilibrium also requires that $N_* > 0$, $S_* > 0$, $I_* > 0$, i.e.,

$$m < eK \frac{\frac{\mu}{\beta}}{\alpha + \frac{\mu}{\beta}} (a + \frac{b\mu}{\beta}) \left[1 - \frac{1}{r} (a + \frac{b\mu}{\beta}) \frac{\mu}{\beta} \right] < m + \mu. \tag{7}$$

Therefore, if the inequality (7) holds, the model (4) has a unique positive equilibrium. Notice that if the model (4) has the positive equilibrium E_* , the steady-state of total predator population $P_* = S_* + I_*$ identically equals $\frac{\mu}{\beta}$ for any given β and μ . Substituting $P_* = \frac{\mu}{B}$ into the inequality (7) gives that

$$\frac{m(\alpha + P_*)}{e(a + bP_*)P_*} < K \left[1 - \frac{1}{r}(a + bP_*)P_* \right] < \frac{(m + \mu)(\alpha + P_*)}{e(a + bP_*)P_*}.$$

It then follows from the expressions of F(P) and G(P) that

$$F\left(\frac{\mu}{\beta}\right) > 0, \quad G\left(\frac{\mu}{\beta}\right) < 0.$$

Therefore, if $F\left(\frac{\mu}{\beta}\right) > 0$ and $G\left(\frac{\mu}{\beta}\right) < 0$ hold, the model (4) has a unique positive equilibrium $E_*(N_*, S_*, I_*)$.

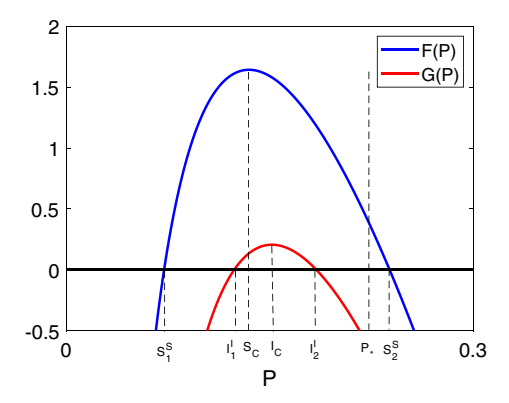
The stability of the equilibria in model (4) is determined by the eigenvalues of its Jacobian matrix. We summarize the results on the existence and stability of these equilibria in Theorem 5.

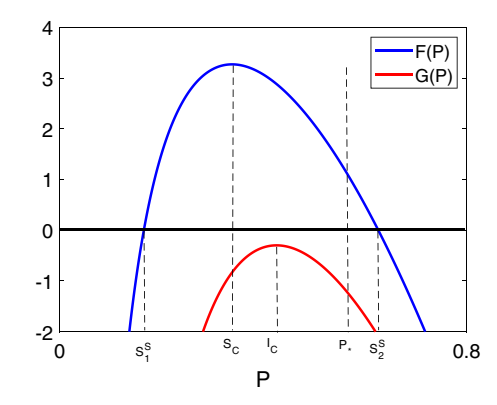
Theorem 5. The model (4) always has two boundary equilibria $E_0(0,0,0)$ and $E_K(K,0,0)$. In addition, the model (4) may have two potential boundary equilibria on the N-S plane and N-I plane and one potential positive equilibrium. Sufficient conditions for the existence and stability of these equilibria are shown in Table 5.

Notes. Above discussions suggest that the existence of boundary equilibria E_1^S , E_2^S , E_1^I , E_2^I has an essential role in the existence of positive equilibrium E_* . We illustrate it by the following two scenarios:

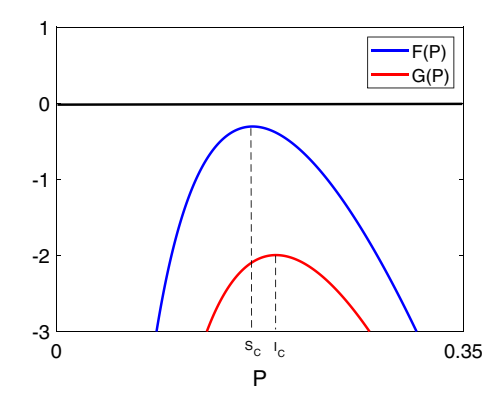
- When $F(S_c) > 0$ and $G(I_c) > 0$, the model (4) has two boundary equilibria E_1^S , E_2^S on the N-S coordinate plane as well as two boundary equilibria E_1^I , E_2^I on the N-I coordinate plane (see Fig. 5(a)). If and only if $I_2^I < \frac{\mu}{\beta} < S_2^S$ or $S_1^S < \frac{\mu}{\beta} < I_1^I$, then the inequalities $F\left(\frac{\mu}{\beta}\right) > 0$, $G\left(\frac{\mu}{\beta}\right) < 0$ hold, i.e., the model (4) has a unique positive equilibrium E_* for any $\frac{\mu}{\beta} \in \left(S_1^S, I_1^I\right)$ or $\left(I_2^I, S_2^S\right)$.
- When $F(S_c) > 0$ and $G(I_c) < 0$, the model (4) only has two boundary equilibria E_1^S , E_2^S on the N-S coordinate plane but no boundary equilibrium on N-I coordinate plane (see Fig. 5(b)). If and only if $S_1^S < \frac{\mu}{\beta} < S_2^S$, then the inequalities $F\left(\frac{\mu}{\beta}\right) > 0$, $G\left(\frac{\mu}{\beta}\right) < 0$ hold, i.e., the model (4) has a unique positive equilibrium for any $\frac{\mu}{\beta} \in \left(S_1^S, S_2^S\right)$.

Above two scenarios suggest that if the function F(P) has no positive root, i.e., $F(S_c) < 0$ holds on the interval $(0, +\infty)$, then the function G(P) also has no positive root since F(P) > G(P), and there does not exist $\frac{\mu}{\beta}$ such that $F\left(\frac{\mu}{\beta}\right) > 0$ and $G\left(\frac{\mu}{\beta}\right) < 0$ (see Fig. 5(c)). It indicates that if the model (4) has no boundary equilibrium on the N-S plane, then it has no boundary equilibrium on the N-I plane or positive equilibrium in the first quadrant.





- (a) Both F(P) = 0 and G(P) = 0 have positive roots
- (b) Only F(P) = 0 has positive roots



(c) Both F(P) = 0 and G(P) = 0 have no positive root

Fig. 5. Three cases for the functions F(P) and G(P) on $(0, +\infty)$. Fig. 5(a) indicates that the model (4) has two boundary equilibria on N-S coordinate plane and two boundary equilibria on N-I coordinate plane. Fig. 5(b) indicates that the model (4) has two boundary equilibria on N-S coordinate plane but has no boundary equilibrium on N-I coordinate plane. Fig. 5(c) indicates that the model (4) has no boundary equilibrium on N-S coordinate plane and N-I coordinate plane.

Numerical investigation and bifurcation diagrams: Based on the above analysis, the predator-prey model (4) can have up to seven equilibria, but it has at most two attractors (bistability) at once. In order to further explore the dynamical patterns of the model (4) with varying key parameters. We take one-parameter and two-parameter bifurcation diagrams to investigate how the mating limitation level α , cooperation coefficient b and disease transmission rate β affect the existence and stability of the positive equilibrium as well as the establishment of disease in the system.

(a) The effects of disease

Fig. 6 illustrates the number and stability of positive equilibrium with two varying parameters. For convenience, we fix r=1, K=10, a=2, b=0.5, e=0.1, m=0.3, $\mu=0.2$ but vary β and α in Fig. 6(a), and fix r=3, K=5, a=0.2, $\alpha=0.2$, e=0.1, m=0.35, $\mu=0.25$ but vary β and b in Fig. 6(b) as two typical examples. Fig. 6(a) suggests that small values of mating limitation α guarantee the existence of positive equilibrium, and the combination with small values of transmission rate β can stabilize the positive equilibrium. The result in Fig. 6(b) suggests that large values of cooperation coefficient b enable the model to have positive equilibrium, and combined with small values of transmission rate β stabilize the system, which means that the disease will be persistent in the system.

Then, we choose $\alpha = 0.25$ and $\alpha = 0.5$ in Fig. 6(a) respectively, and take the additional bifurcation diagrams of the positive equilibrium as well as the boundary equilibria E_1^S , E_2^S , E_1^I , E_2^I with respect to β as shown in Fig. 7. The other parameter values are the same as in Fig. 6(a).

For $\alpha = 0.25$ (see Fig. 7(a) and (c)): When β is small (see the region A_{ns}), there are two boundary equilibria E_1^S , E_2^S where E_1^S is unstable and E_2^S is locally stable, and there are also two boundary equilibria E_1^I , E_2^I where both of them are unstable;

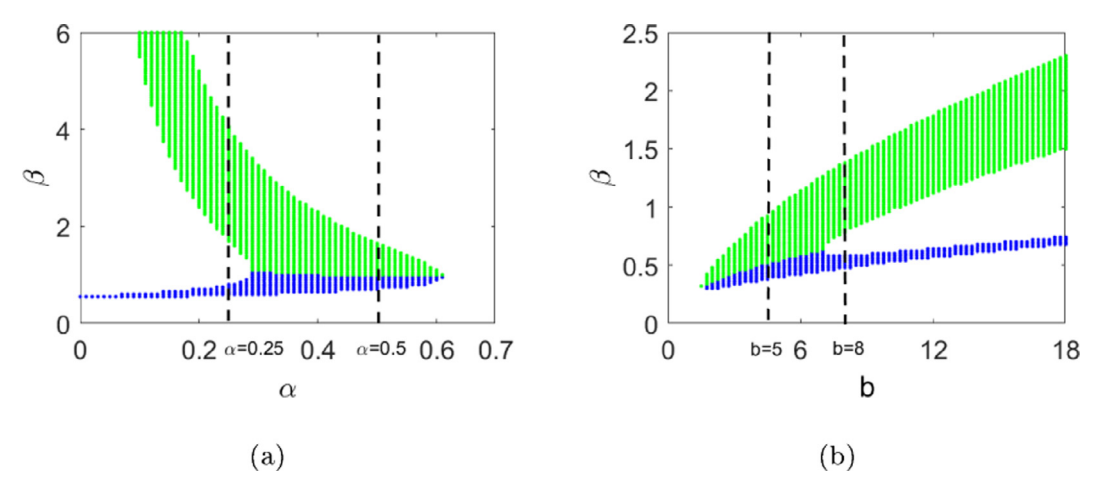


Fig. 6. Two parameter bifurcation diagrams in $\alpha - \beta$ plane and $b - \beta$ plane respectively. Fig. 6(a) describes the number and stability of positive equilibrium of model (4) with varying α and β , and the other values of parameters are: r = 1, K = 10, a = 2, b = 0.5, e = 0.1, m = 0.3, $\mu = 0.2$. Fig. 6(b) describes the number and stability of positive equilibrium of model (4) with varying b and b, and the other values of parameters are: b = 0.1, b = 0.2, b = 0.1, b = 0.2. In blue regions, the unique positive equilibrium is stable; in green regions, the unique positive equilibrium is unstable; in the white regions, the model has no positive equilibrium.

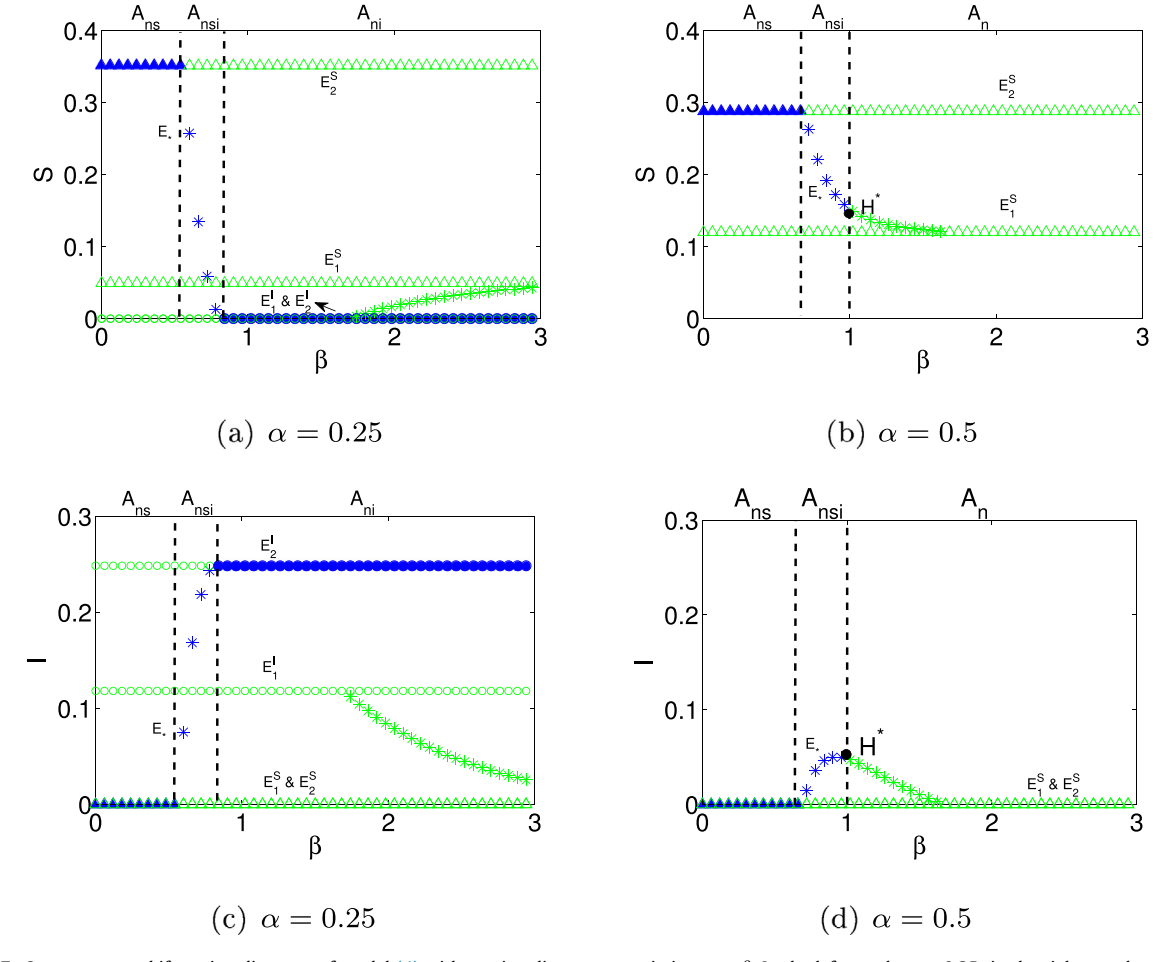


Fig. 7. One parameter bifurcation diagrams of model (4) with varying disease transmission rate β . In the left panels, $\alpha = 0.25$; in the right panels, $\alpha = 0.5$. The boundary equilibria E_1^{c} , E_2^{c} are denoted by triangle, the boundary equilibria E_1^{c} , E_2^{c} are denoted by small circle, and the positive equilibrium E_* is denoted by asterisk. Blue markers (green markers) represent that the equilibria are stable (unstable). H denotes the Hopf bifurcation point. In area A_{ns} , only prey and susceptible predator can coexist stably; in area A_{ns} , only prey and infected predator can coexist stably; in area A_{ns} , only prey exists in system.

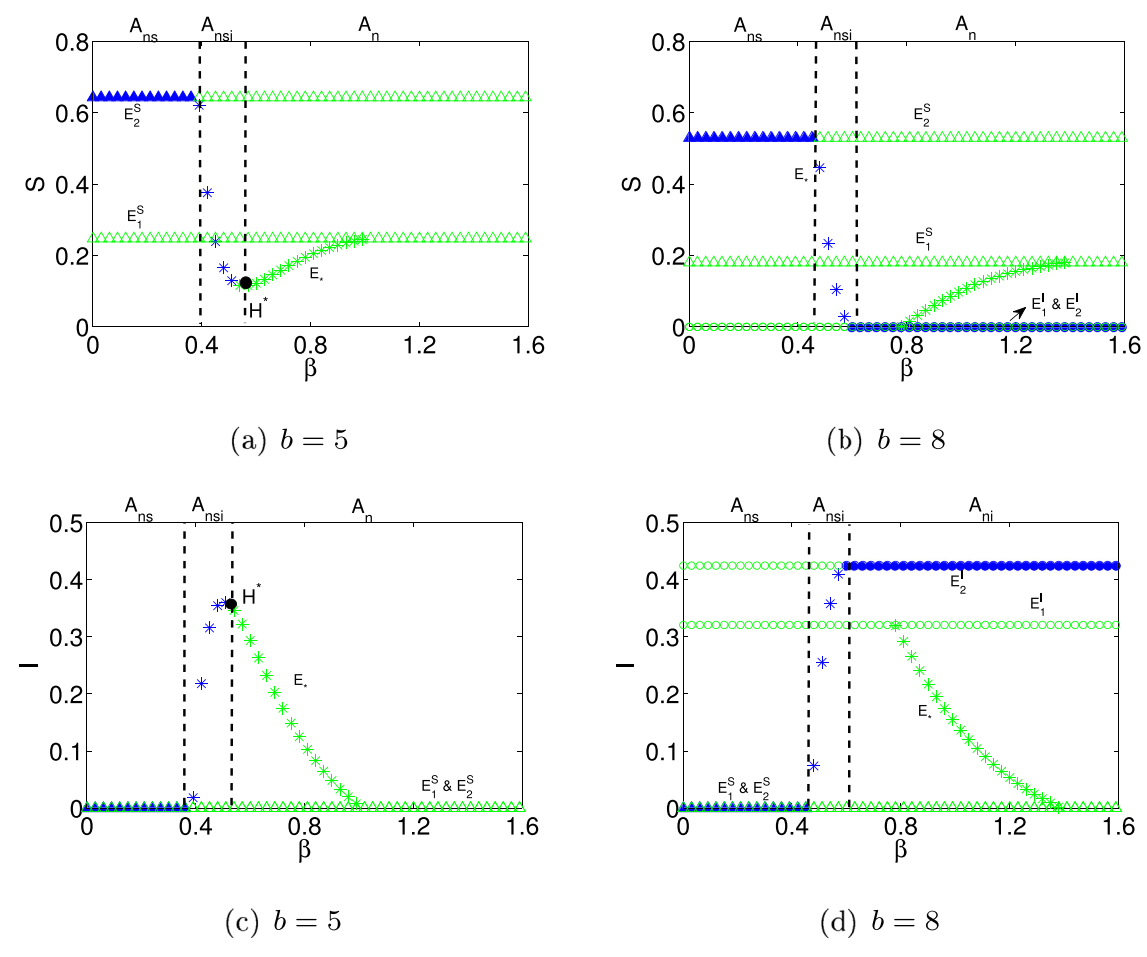


Fig. 8. One parameter bifurcation diagrams of model (4) with varying disease transmission rate β. In the left panels, b = 5; in the right panels, b = 8. The boundary equilibria E_1^5 , E_2^5 are denoted by triangle, the boundary equilibria E_1^1 , E_2^1 are denoted by small circle, and the positive equilibrium E_* is denoted by asterisk. Blue markers (green markers) represent that the equilibria are stable (unstable). H denotes the Hopf bifurcation point. In area A_{ns} , only prey and susceptible predator can coexist stably; in area A_{ns} , only prey and infected predator can coexist stably; in area A_{ns} , only prey exists in system.

As β increases (see the region A_{nsi}), the stable boundary equilibrium E_2^S becomes unstable and a stable positive equilibrium E_* appears; Further increasing β stabilizes the boundary equilibria E_2^I and enables the positive equilibrium E_* to disappear (see the region A_{ni}); If β continues to increase, the model has positive equilibrium E_* again which remains unstable.

For $\alpha = 0.5$ (see Fig. 7(b) and (d)): When β is small (see the region A_{ns}), the model only has two boundary equilibria E_1^S , E_2^S where E_2^S is stable and E_1^S is unstable; as β continues to increase (see the region A_{nsi}), the boundary equilibrium E_2^S becomes unstable, and the model has a stable positive equilibrium E_* ; Then further increasing β destabilizes the positive equilibrium and leads to a Hopf bifurcation, and further increasing drives the positive equilibrium to disappear (see the region A_{nsi}).

Biological implications: Fig. 7 suggests that when the mating limitation is weak, increasing the disease transmission rate promotes the disease to establish itself in the system and further increasing drives all the susceptible predator but not infected ones to extinct; While when the mating limitation is strong, large value of the disease transmission rate drives the whole predator population to die out and only preys are left in the system.

We also choose b = 5 and b = 8 in Fig. 6(b), and take additional bifurcation diagrams to explore insights into the dynamical patterns of disease establishment in the system by varying transmission rate under the different cooperation coefficient b. The results are illustrated in Fig. 8, which is very similar to Fig. 7. Therefore, we summarize the biological implications of Fig. 8 directly.

Biological implications: When the hunting cooperation is weak, increasing the disease transmission rate enables the disease to persist in the system, further increasing drives the whole predator population to die out and leaves only the prey to survive; When the hunting cooperation is strong, large values of the transmission rate drive all the susceptible predator to extinct.

(b) The effects of hunting cooperation

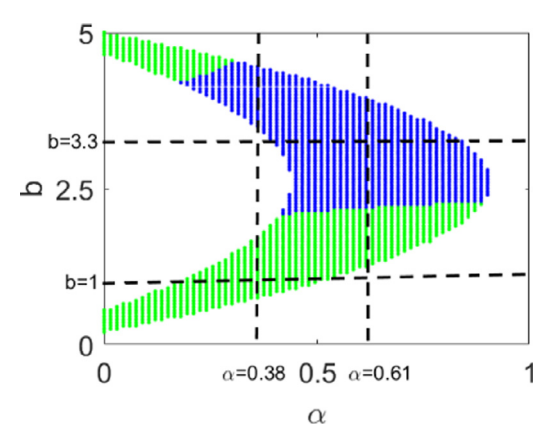


Fig. 9. Two parameters bifurcation diagrams for the existence of positive equilibrium of model (4). We fix r = 1.5, K = 5, a = 0.2, e = 0.15, m = 0.2, $\mu = 0.1$, $\alpha = (0, 5)$, b = (0, 15). In blue region, the positive equilibrium is stable; in green region, the positive equilibrium is unstable.

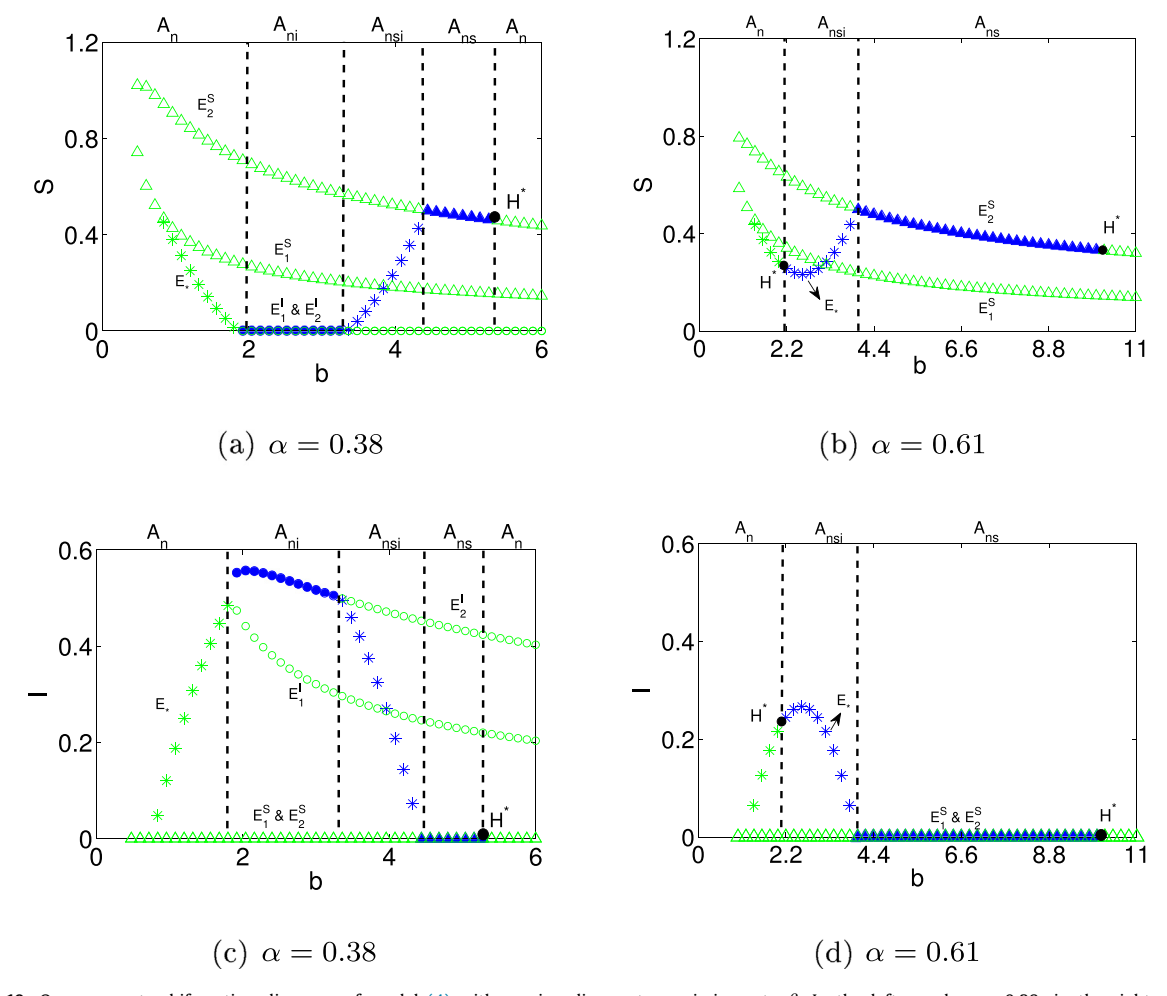


Fig. 10. One parameter bifurcation diagrams of model (4) with varying disease transmission rate β. In the left panels, α = 0.38; in the right panels, α = 0.61. The boundary equilibria E_1^{ς} , E_2^{ς} are denoted by triangle, the boundary equilibria E_1^{ς} , E_2^{ς} are denoted by small circle, and the positive equilibrium E_* is denoted by asterisk. Blue markers (green markers) represent that the equilibria are stable (unstable). H denotes the Hopf bifurcation point. In area A_{ns} , only prey and susceptible predator can coexist stably; in area A_{ns} , only prey and infected predator can coexist stably; in area A_{ns} , only prey exists in system.

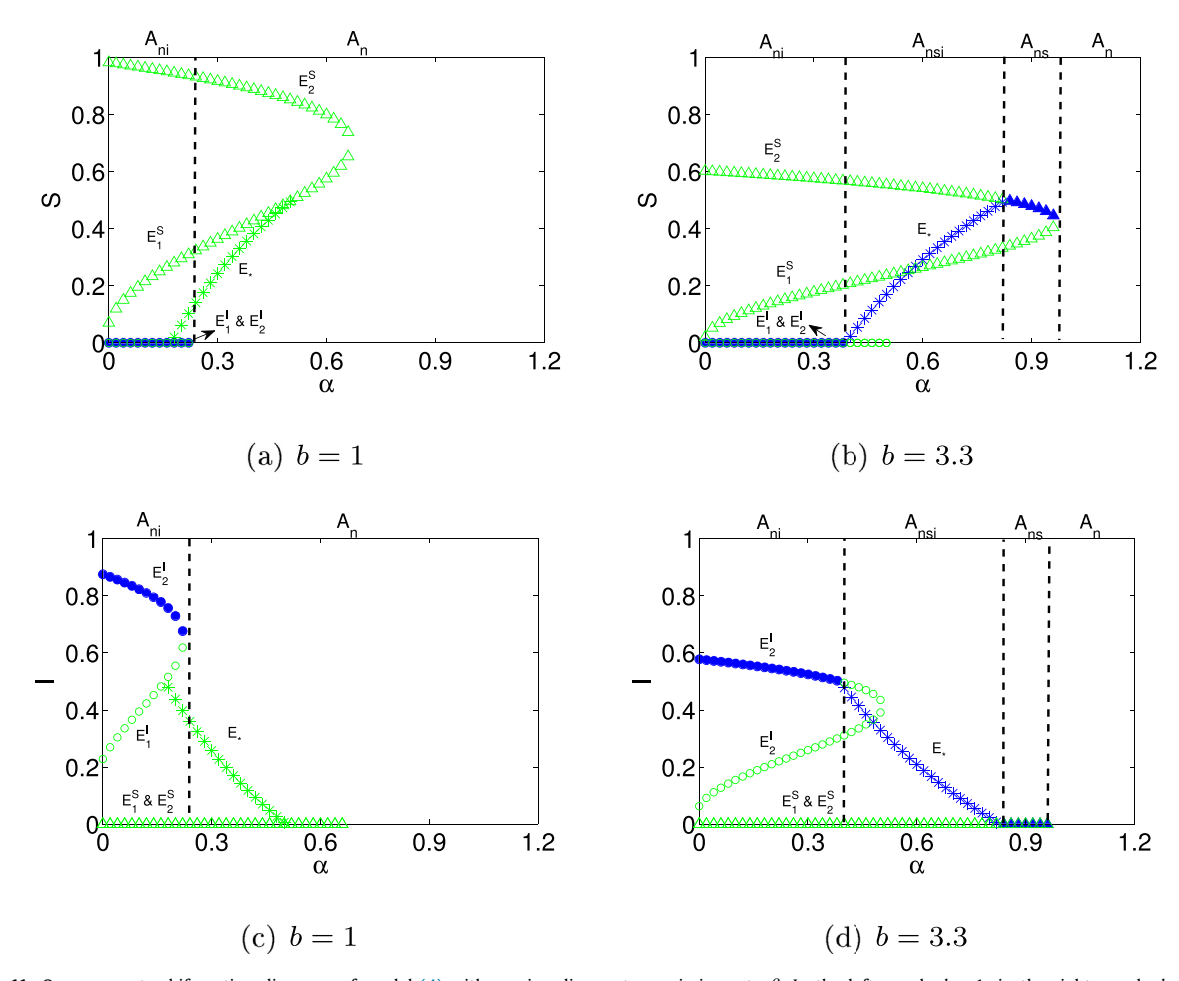


Fig. 11. One parameter bifurcation diagrams of model (4) with varying disease transmission rate β. In the left panels, b = 1; in the right panels, b = 3.3. The boundary equilibria E_1^S , E_2^S are denoted by triangle, the boundary equilibria E_1^I , E_2^I are denoted by small circle, and the positive equilibrium E_* is denoted by asterisk. Blue markers (green markers) represent that the equilibria are stable (unstable). H denotes the Hopf bifurcation point. In area A_{ns} , only prey and susceptible predator can coexist stably; in area A_{ns} , only prey and infected predator can coexist stably; in area A_{ns} , only prey exists in system.

Next, we fix r = 1.5, K = 5, a = 0.2, $\beta = 0.2$, e = 0.15, m = 0.2, $\mu = 0.1$ as another typical example, and perform the two-parameter bifurcation of mating limitation α and hunting cooperation coefficient b. The results presented in Fig. 9 provide insights into the effects of α and b on the existence and stability of coexistence equilibrium. Fig. 9 suggests that large values of b combined with small values of α guarantee the existence of positive equilibrium which could be stable when b is large enough.

We choose $\alpha = 0.38$ and $\alpha = 0.61$ in Fig. 9, respectively, and perform the additional one-parameter bifurcation diagrams to explore the dynamical patterns of model (4) with varying hunting cooperation b under different level of mating limitation. The simulated results are presented in Fig. 10.

For $\alpha=0.38$ (see Fig. 10(a) and (c)): When b is small (see region A_n), the model (4) has one positive equilibrium E_* and two boundary equilibria E_1^S , E_2^S , and all of them are unstable; As b increases (see region A_{ni}), the positive equilibrium disappears, and the model exhibits two boundary equilibria E_1^I , E_2^I where E_1^I is a saddle and E_2^I is locally stable; as b continues to increase, the boundary equilibrium E_2^I loses its stability, and the positive equilibrium appears again and keeps stable as varying b (see region A_{nsi}); As b further increases (see region A_{ns}), the positive equilibrium disappears, and the boundary equilibrium E_2^S becomes stable; When the value of b is too large, the system loses stability and leads to a Hopf bifurcation.

For $\alpha = 0.61$ (see Fig. 10(b) and (d)): When b is small (see region A_n), the model (4) has one positive equilibrium E_* and two boundary equilibria E_1^S , E_2^S , and all of them are unstable; As b increases, the system exhibits a Hopf bifurcation and the positive equilibrium becomes stable (see region A_{nsi}); as b continues to increase (see region A_{ns}), the positive equilibrium disappears and the boundary equilibrium E_2^S becomes stable; Further, too large values of b destabilizes the stability of system and leads to a Hopf bifurcation again.

Biological implications: When the mating limitation is weak, increasing the cooperation coefficient saves the predators from extinction and leaves only infected ones to coexist with prey, further increasing enables the disease to establish in

the system successfully, and further increasing cooperation drives the disease to extinct and leaves the healthy predators to coexist with prey; When the mating limitation is strong, increasing the hunting cooperation coefficient saves all the predators from extinction and enables the disease to establish in the system, and further increasing drives the disease extinct and leaves the healthy predator to coexist with prey.

(c) The effects of mating limitation

In order to get insights into how the mating limitation affect on the stability of model (4) under different cooperation coefficients, we also implement additional one-parameter bifurcation diagrams of mating limitation α as shown in Fig. 11. For convenience, we fix b=1 in Fig. 11(a), (c) and b=3.3 in Fig. 11(b), (d) respectively, and the values of other parameters are the same as in Fig. 9.

For b=1 (see Fig. 11(a) and (c)): When α is small (see region A_{ni}), the model has four boundary equilibria E_1^S , E_2^S , E_1^I , E_2^I , where E_2^I is locally stable while the others are unstable; As α increases, the positive equilibrium E_* appears first and then disappears, which is always unstable; The boundary equilibria E_1^S , E_2^S as well as the boundary equilibria E_1^I , E_2^I also disappear as varying α (see region A_n).

For b=3.3 (see Fig. 11(b) and (d)): When α is small (see region A_{ni}), the model has four boundary equilibria E_1^S , E_2^S , E_1^I , E_2^I , and E_2^I is locally stable while the others are unstable; Further increasing α destabilizes the boundary equilibrium E_2^I and enables the model to have a positive equilibrium E_* which is always locally stable (see region A_{nsi}); as α continues to increase (see region A_{ns}), the positive equilibrium, as well as the boundary equilibria E_2^I , disappear from the system, and the boundary equilibrium E_2^S becomes stable; Further, too large values of α drives all the equilibria to extinct (see region A_n).

Biological implications: For the scenario that the infectious disease has depleted the susceptible predators which have low strength of cooperation, increase mating limitation drives the whole predator population to die out; When the predators have high level of cooperation, increasing mating limitation parameter saves the healthy predators from dying out, further increasing drives the disease to extinct from the system, but too strong mating limitation drives all the predators to go extinction and leaves only the prey to survive.

5. Conclusion

Allee effect has great impacts on species' establishment, persistence, invasion and evolution. Many mathematical models have investigated the impact of the Allee effect as well as the joint effects which incorporate both the Allee effect and disease on the interspecific relationships in the predator-prey model [12–14,44–47]. Recently, Hilker et al. explored a predator-prey model with cooperative hunting behavior in predators [30]. They found that hunting cooperation within the right scope can mediate the survival of predators which can not exist in the system in the absence of cooperation. They also study the effect of disease on the predator-prey model with predator subject to hunting cooperation [28]. The result indicates that predators with strong cooperation are 'immune' to disease-induced host extinction. In this paper, we propose a predator-prey model with group living predators subject to mating limitation and disease. There are three unique features of our assumptions: (a) disease has a vertical transmission, and it can cause additional mortality in infected; (b) Allee effect induced by mating limitation is built in the reproduction of predators, and the disease has little effect on it; (c) the predators capture food through cooperation, and the disease has little effect on this behavior. The theoretical results and numerical simulations on the proposed model provide insights into the effects of the disease, hunting cooperation and mating limitation on the model's dynamical pattern. We summarize our main results and their related biological implications as follows:

- Based on our assumptions, we propose an eco-epidemiological model described by ODE Eq. (4). Theorem 1 provides the positivity and boundedness of this model.
- The theoretical results in Theorems 2–4 combined with bifurcation diagrams in Figs. 1, 2, 4 provide us a full picture on the dynamics of the disease-free model with or without mating limitation and hunting cooperation. By comparing to the classical predator-prey model, when the mating limitation parameter of predator is greater than zero, the model must exhibit a predator extinction equilibrium which is always locally stable. From the biological explanation, the predator population will die out if its initial density is small. Moreover, we can conclude the impacts of mating limitation and hunting cooperation on the predator-prey model: (a) the mating limitation can generate strong Allee effect when its parameter α is not large; (b) increasing the mating limitation parameter α can reduce the size of predator population and stabilize the system, but too large values can lead to the extinction of the predators; (c) when the predators fail to produce offspring, the enhancement of hunting cooperation can guarantee the predator to survive in the system and generate a strong Allee effect; (d) increasing the hunting cooperation coefficient b can reduce the size of predator population, but too large would destabilize the system and lead to a Hopf bifurcation.
- Theorem 5 provides the local dynamics of full model (4), and it indicates that if the model (4) has no boundary equilibrium on the N-S plane, then it has no positive equilibrium and boundary equilibrium on the N-I plane. One-parameter and two-parameter bifurcations are presented to obtain how the interplay among disease, mating limitation, hunting cooperation can affect the persistence of species in the system. Numerical simulations in Fig. 6–8 suggest that: (a) when the mating limitation parameter is small or the hunting cooperation coefficient is large, the disease can drive the susceptible predators to extinction and leave infected ones to survive with prey in the system; (b) when the mating limitation parameter is large or the hunting cooperation coefficient is small, the disease can drive the extinction of the whole

predator population. Numerical simulations in Figs. 9, 10 suggest that the hunting cooperation can drive the disease among predators to go extinction and guarantee the coexistence between predator and prey. Numerical simulations in Figs. 9, 11 suggest that the mating limitation can save the predator from disease-driven extinction and lead the disease to disappear from the system when the cooperation coefficient is large, while it also drives the whole predator population to die out if the cooperation coefficient of predators is small.

Our results can provide a new perspective on population protection and disease control, by intervening in the species' cooperative behavior or mating success rate. This may be helpful in establishing an effective control strategy for epidemic disease. But, in reality, there must be more complex population relationships in ecological communities. Therefore, it is meaningful to incorporate other ingredients, such as different compartmental structures. It will also be interesting to generalize our model by considering more complex laws of disease transmission, such as different incidence or a fraction of newborns that can be infected from the parent. All these questions could be further discussed. We leave these for future investigations.

Declaration of Competing Interest

The authors declare that they have no conflict of interest.

Acknowledgments

L. Wang is partially supported by the Scholarship Foundation of China Scholarship Council (Award Number 201906840071); and the Practice Innovation Program of Jiangsu Province (KYCX19_0255). Z. Qiu is partially supported by the National Natural Science Foundation of China (12071217, 11971232, 11671206). T. Feng is partially supported by the Outstanding Chinese and Foreign Youth Exchange Program of China Association of Science and Technology; and the Scholarship Foundation of China Scholarship Council (Award Number 201806840120). Y. Kang is partially supported by the NSF-DMS (1716802); the NSF- IOS/DMS (1558127); the DARPA -SBIR 2016.2 SB162-005 Phase II; and the James S. McDonnell Foundation 21st Century Science Initiative in Studying Complex Systems Scholar Award (UHC Scholar Award 220020472).

Appendix A. Proof of Theorem 1

For any $N \ge 0$, $S \ge 0$, $I \ge 0$, we have

$$\left. \frac{dN}{dt} \right|_{N=0} = 0, \quad \left. \frac{dS}{dt} \right|_{S=0} = 0, \quad \left. \frac{dI}{dt} \right|_{I=0} = 0,$$

which implies that N = 0, S = 0, I = 0 are invariant manifolds. It then follows that the model (4) is positively invariant in \mathbb{R}^3_+ . Since

$$\frac{dN}{dt} = rN\left(1 - \frac{N}{K}\right) - \left[a + b(S+I)\right]N(S+I) \le rN\left(1 - \frac{N}{K}\right),$$

it is easy to see that

$$\limsup N(t) \leq K.$$

Define Z(t) = N(t) + S(t) + I(t), and the derivative of Z(t) is

$$\frac{dZ}{dt} \leq -mZ + M$$

where $M = \frac{K(r+m)^2}{4r}$. By using the comparison principle, we have

$$Z(t) \leq \frac{M}{m} + \left(Z(t_0) - \frac{M}{m}\right)e^{-m(t-t_0)}.$$

It is easy to get that $Z(t) \leq \frac{M}{m}$ as $t \to +\infty$. Thus, all solutions of (4) starting in \mathbb{R}^3_+ will remain within the region

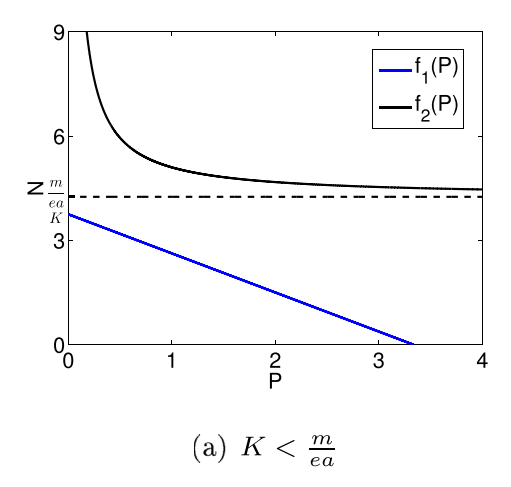
$$\bar{\Omega} = \{(N, S, I) \in \mathbb{R}^3_+ : 0 \le N \le K, 0 \le N + S + I \le \frac{M}{m}\}.$$

Appendix B. Proof of Theorem 2

Straightforward computation yields that the model (5) always has two boundary equilibria $E_0(0,0)$, $E_K(K,0)$. Let $f_1(P) = K - \frac{K}{R}aP$, $f_2(P) = \frac{m\alpha}{eaP} + \frac{m}{ea}$. Depending on the values of parameters, the equation $f_1(P) = f_2(P)$ may have none or two positive roots which are illustrated in Fig. 12. The positive equilibrium of model (5) is completely determined by the positive roots of $f_1(P) - f_2(P) = 0$.

Simple calculation yields that the function $f_1(P) - f_2(P)$ has solutions

$$P_{1,2} = \frac{(eaK-m) \pm \sqrt{(m-eaK)^2 - 4\frac{K}{r}ea^2m\alpha}}{2\frac{K}{r}ea^2}.$$



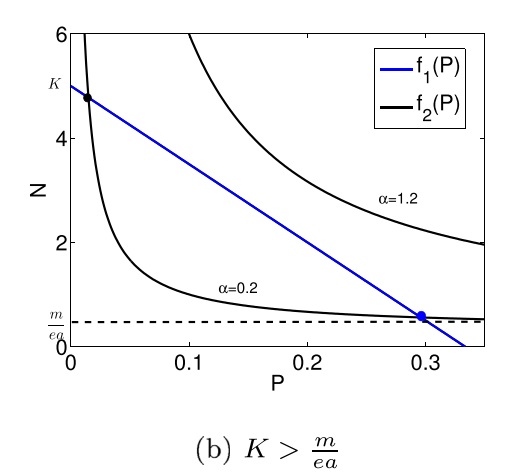


Fig. 12. Nullclines for model (5). The dotted line is $\frac{m}{ea}$, the blue line is $f_1(P)$, and the black line is $f_2(P)$. Fig. 12(a) indicates that the model has zero positive equilibrium, Fig. 12(b) indicates that the model has zero or two positive equilibria.

If eaK - m > 0 and $(m - eaK)^2 - 4\frac{K}{r}ea^2m\alpha > 0$, then P_1 and P_2 are two real positive roots. It then follows that

$$N_{1,2}=K-\frac{(eaK-m)\pm\sqrt{(m-eaK)^2-4\frac{K}{r}ea^2m\alpha}}{2ea}>0$$

since $N = \frac{\alpha + P}{eaP}$. Therefore, the model has two positive equilibria $E_1^*(N_1^*, P_1^*)$ and $E_2^*(N_2^*, P_2^*)$ if $\frac{Kea}{m} > 1$ and $\alpha < \frac{(m - eaK)^2 r}{4ea^2 mK}$. Next, we investigate the local stability of these equilibria. The Jacobin matrix can be expressed as

$$J = \begin{bmatrix} r(1 - \frac{2}{K}N) - aP & -aN \\ ea\frac{P}{\alpha + P}P & -m + eaN\frac{P}{\alpha + P}\left(1 + \frac{\alpha}{\alpha + P}\right) \end{bmatrix}.$$

It is easy to obtain that the Jacobin matrix at E_0 has two eigenvalues $\lambda_1 = r$, $\lambda_2 = -m$. Thus, the boundary equilibrium E_0 is unstable. Similarly, the Jacobin matrix at E_K has two eigenvalues $\lambda_1 = -r$, $\lambda_2 = -m$, i.e., the boundary equilibrium E_K is locally asymptotically stable.

Let $E_{\#}(N_{\#}, P_{\#})$ be any positive equilibrium $E_1^*(N_1^*, P_1^*)$ or $E_2^*(N_2^*, P_2^*)$ where $P_1^* < P_2^*$. After extensive algebraic calculations, the corresponding characteristic equation at $E_{\#}$ is

$$f(\lambda) = \lambda^2 + A_1(N_\#, P_\#)\lambda + A_2(N_\#, P_\#) = 0,$$
(B.1)

where $A_1(E_\#) = \frac{r}{K}N_\# - m\frac{\alpha}{\alpha + P_\#}$, $A_2(E_\#) = -\frac{mr}{aK}(f_1'(P_\#) - f_2'(P_\#))$. Let $\lambda_1(E_\#)$, $\lambda_2(E_\#)$ be the roots of (B.1), and assume that $\Re \lambda_1(E_\#) \leq \Re \lambda_2(E_\#)$. Since $f_1'(P_1^*) - f_2'(P_1^*) > 0$ and $f_1'(P_2^*) - f_2'(P_2^*) < 0$ (see Fig. 12(b)), it then follows that $\lambda_1(E_1^*)\lambda_2(E_1^*) = A_2(E_1^*) < 0$, $\lambda_1(E_2^*)\lambda_2(E_2^*) = A_2(E_2^*) > 0$. This means that $\Re \lambda_1(E_1^*) < 0 < \Re \lambda_2(E_1^*)$. Therefore, the positive equilibrium E_1^* is a saddle when it exists. The stability of the positive equilibrium E_2^* is further determined by the sign of $\lambda_1(E_2^*) + \lambda_2(E_2^*) = -A_1(E_2^*)$. If $A_1(E_2^*) > 0$, i.e., $\frac{r}{K} > ea\frac{\alpha P_2^*}{(\alpha + P_2^*)^2}$, then we have $\Re \lambda_1(E_2^*) \leq \Re \lambda_2(E_2^*) < 0$, and the positive equilibrium E_2^* is locally asymptotically stable; if $A_1(E_2^*) < 0$, i.e., $\frac{r}{K} < ea\frac{\alpha P_2^*}{(\alpha + P_2^*)^2}$, then we have $0 < \Re \lambda_1(E_2^*) \leq \Re \lambda_2(E_2^*)$, and the positive equilibrium E_2^* is unstable.

Appendix C. Proof of Theorem 3

Straightforward computation yields that the model (1) always has two boundary equilibria $E_0(0,0)$, $E_K(K,0)$. Let $f_1(P) = K - \frac{K}{r}(a+bP)P$, $f_2(P) = \frac{m}{e(a+bP)}$. The positive roots of $f_1(P) = f_2(P)$ are illustrated as shown in Fig. 13. Define

$$\begin{split} G(P) &= e(a+bP)(f_2(P)-f_1(P)), \\ &= \frac{b^2 eK}{r} P^3 + \frac{2abeK}{r} P^2 + eK(\frac{a^2}{r}-b)P + (m-eaK). \end{split}$$

Any positive equilibrium must satisfy the function G(P) = 0. Derivation of the function G(P) gives that

$$G'(P) = \frac{3b^2eK}{r}P^2 + \frac{4abeK}{r}P + eK(\frac{a^2}{r} - b).$$

The above function provides a property that there are two extreme points P_L and P_R such that the function G(P) reaches its first hump (maximum) at P_L and second hump (minimum) at P_R , where P_L is always negative and P_R is positive if $\frac{a^2}{r} - b < 0$. It suggests that:

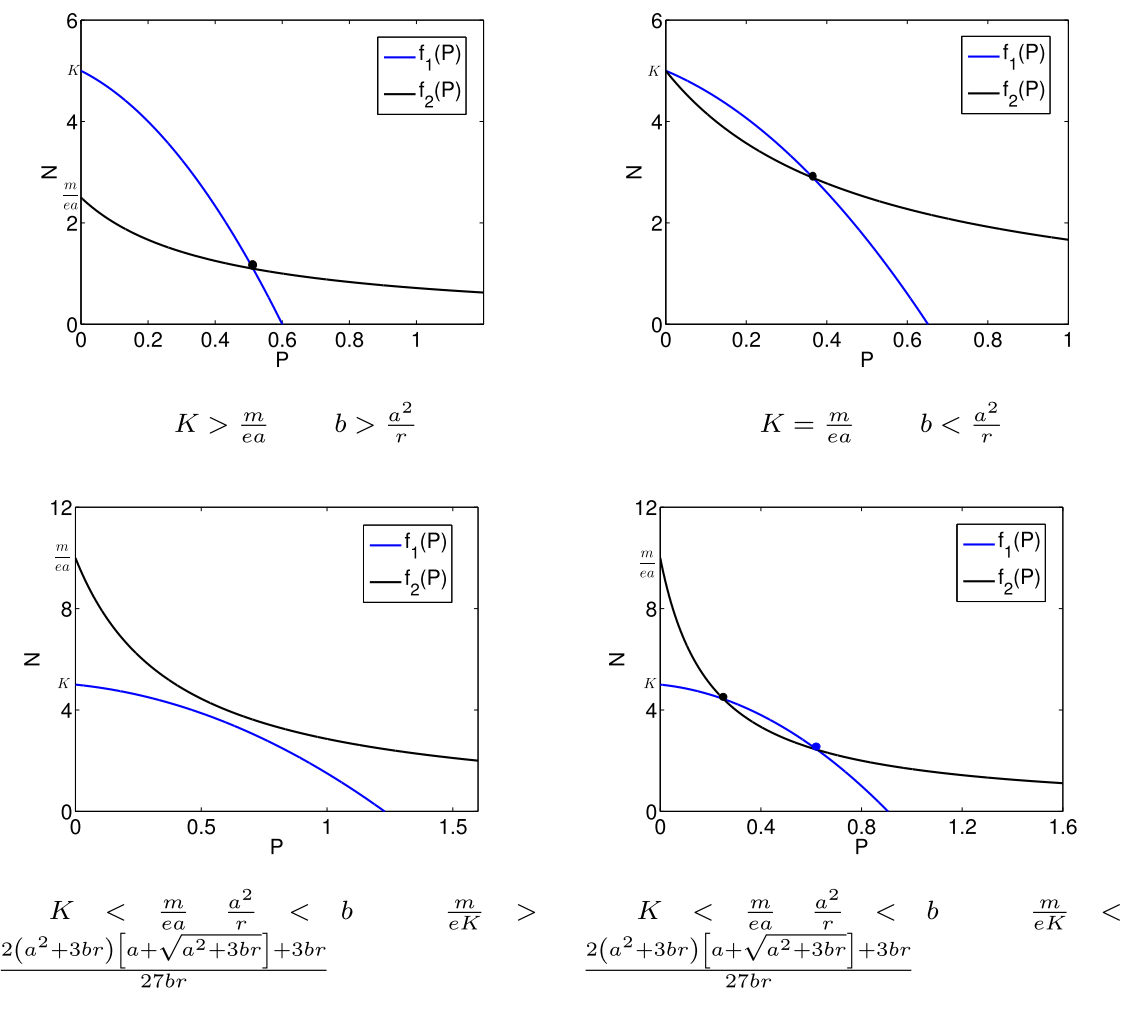


Fig. 13. Nullclines for model (1). The blue line is $f_1(P)$, and the black line is $f_2(P)$. Fig. 13(a) and 13(b) indicates that the model has unique equilibrium. Fig. 13(c) indicates that the model has zero equilibrium. Fig. 13(d) indicates that the model has two equilibria.

- 1. when $\frac{Kea}{m} > 1$, G(P) = 0 has one positive root, and the model (1) has one positive equilibrium; 2. when $\frac{Kea}{m} = 1$, G(P) = 0 has one positive root if $\frac{a^2}{r} b < 0$, and the model (1) has one positive equilibrium $E_*(N_*, P_*)$;
- 3. when $\frac{Kea}{m} < 1$, G(P) = 0 can have two positive roots if $\frac{a^2}{r} b < 0$ and $G(P_R) < 0$ (i.e., $\frac{m}{eK} < \frac{2(a^2 + 3br)[a + \sqrt{a^2 + 3br}] + 3br}{27br}$). Therefore, the model (1) has two positive equilibria $E_1^*(N_1^*, P_1^*)$ and $E_2^*(N_2^*, P_2^*)$.

Next, we explore the stability of the equilibria of model (1), and the Jacobin matrix is

$$J = \begin{bmatrix} r(1-\frac{2}{K}N) - (a+bP)P & -N(a+2bP) \\ e(a+bP)P & -m+eN(a+2bP) \end{bmatrix}.$$

It is easy to obtain that the Jacobin matrix at E_0 has two eigenvalues $\lambda_1 = r$, $\lambda_2 = -m$. Thus, the boundary equilibrium E_0 is unstable. Similarly, the Jacobin matrix at E_K has two eigenvalues $\lambda_1 = -r$, $\lambda_2 = eaK - m$, and we know that the boundary equilibrium E_K is always locally stable if eaK < m and unstable of eaK > m.

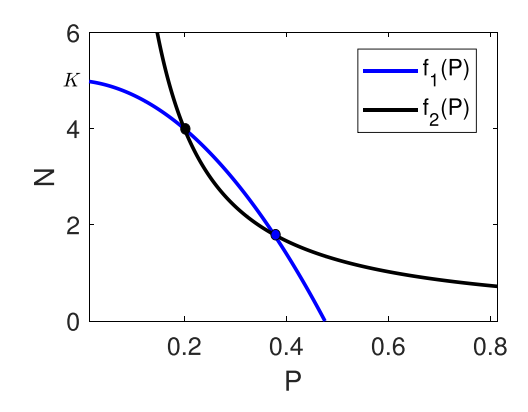
Let $E_{\#}(N_{\#}, P_{\#})$ be any positive equilibrium. The characteristic equation of $E_{\#}$ is

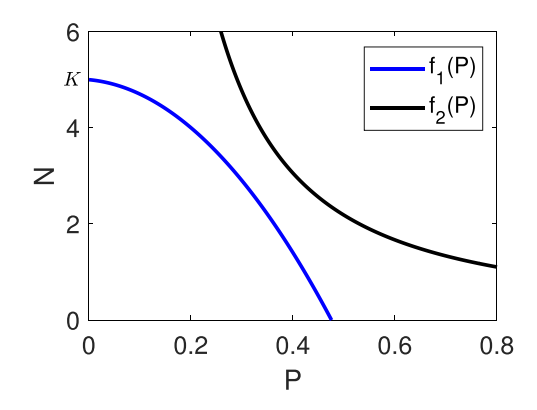
$$f(\lambda) = \lambda^2 + A_1(N_{\#}, P_{\#})\lambda + A_2(N_{\#}, P_{\#}) = 0, \tag{9}$$

where

$$A_1(E_\#) = -(\lambda_1 + \lambda_2) = \frac{r}{K}N_\# - ebN_\#P_\#,$$

$$A_2(E_\#) = \lambda_1 \lambda_2 = -\frac{r}{K} N_\# P_\# (f_1'(P_\#) - f_2'(P_\#)).$$





- (a) Model (3) has two positive equilibria
- (b) Model (3) has none positive equilibrium

Fig. 14. Nullclines for model (3). The horizontal dotted line is $\frac{m}{pq}$, the blue dot is the positive equilibrium with larger predator density P_2^* , and the black dot is the positive equilibrium with smaller predator density P_1^* .

Let $\lambda_1(E_{\pm})$, $\lambda_2(E_{\pm})$ be the roots of (9), and assume that $\Re \lambda_1(E_{\pm}) \leq \Re \lambda_2(E_{\pm})$. Then by using the same arguments as the proof in Appendix B, we can obtain the stability of model (1) easily. We conclude the results as follows:

- 1. When the model (1) has one positive equilibrium E_* , the positive equilibrium E_* is locally asymptotically stable if $\frac{r}{V}$ > ebP_* , and the positive equilibrium E_* is source if $\frac{r}{K} < ebP_*$.
- 2. When the model has two positive equilibria E_1^* , E_2^* , we have that the positive equilibrium E_1^* is a saddle, the positive equilibrium E_2^* is locally asymptotically stable if $\frac{r}{K} > ebP_2^*$ and the positive equilibrium E_2^* is a source if $\frac{r}{K} < ebP_2^*$.

Appendix D. Proof of Theorem 4

Straightforward computation yields that the model (3) always has two boundary equilibria $E_0(0,0)$, $E_K(K,0)$. Let $f_1(P)=$ $K - \frac{K}{r}(a+bP)P$, $f_2(P) = \frac{m(\alpha+P)}{e(a+bP)P}$. The number of positive equilibrium of model (3) is determined by the number of positive roots of the equation $f_1(P) - f_2(P) = 0$ which is shown in Fig. 14. In the following, we only consider the positive roots of equation that

$$\begin{split} H(P) = & \frac{r}{4eb^2K} (f_1(P) - f_2(P)), \\ = & \frac{1}{4} P^4 + \frac{a}{2b} P^3 + \frac{a^2 - br}{4b^2} P^2 + \frac{(m - eaK)r}{4eb^2K} P + \frac{\alpha mr}{4eb^2K}. \end{split}$$

Then, we have

$$H'(P) = P^3 + \bar{b}P^2 + \bar{c}P + \bar{d}$$

where $\bar{b} = \frac{3a}{2b} > 0$, $\bar{c} = \frac{a^2 - br}{2b^2}$, $\bar{d} = \frac{(m - eaK)r}{4eb^2K}$. It then follows that

$$H''(P) = 3P^2 + 2\bar{b}P + \bar{c}$$

which has two real solutions

$$\gamma_1 = \frac{-\bar{b} - \sqrt{\bar{b}^2 - 3\bar{c}}}{3}, \quad \gamma_2 = \frac{\bar{b} + \sqrt{\bar{b}^2 - 3\bar{c}}}{3}$$

since $\bar{b}^2 - 3\bar{c} > 0$. It is easy to get that the function H(P) has two positive roots if one of the following conditions holds:

1.
$$m - eaK < 0$$
 and $H(\eta) < 0$, where η is the largest positive real root of $H'(P) = 0$;
2. $m - eaK > 0$, $b > \frac{a^2}{r}$, $H'(\gamma_2) < 0$ and $H(\eta) < 0$, where η is the largest positive real root of $H'(P) = 0$.

To obtain the sufficient conditions for the existence of positive real roots of H(P) = 0, we only need to find the largest positive root η . For convenience, we take a linear transformation of H'(P)=0 and it becomes

$$H'(P) = P^3 + kP + q,$$

where $k = \bar{c} - \frac{\bar{b}^2}{3}$, $q = \frac{2}{27}\bar{b}^3 - \frac{1}{3}\bar{b}\bar{c} + \bar{d}$. By using Cardano's Formula, we obtain that:

- 1. When k < 0 and $H'(\gamma_1) < 0$, the positive real root η is $g + \sqrt[3]{A} + \sqrt[3]{B}$,
- 2. When k < 0 and $H'(\gamma_1) = 0$, the positive real root η is $g + \frac{2}{3}\sqrt{-3k}$,

3. When k < 0 and $H'(\gamma_1) = 0$, the positive real root η is $g + \omega^2 \sqrt[3]{A} + \omega \sqrt[3]{B}$,

where $g = -\frac{\bar{b}}{3}$, $A = -\frac{q}{2} + \sqrt{\left(\frac{q}{2}\right)^2 + \left(\frac{k}{3}\right)^3}$, $B = -\frac{q}{2} - \sqrt{\left(\frac{q}{2}\right)^2 + \left(\frac{k}{3}\right)^3}$, $\omega = -\frac{1}{2} + \frac{\sqrt{3}}{2}i$. Therefore, the model (3) has two positive equilibria $E_1^*(N_1^*, P_1^*)$ and $E_2^*(N_2^*, P_2^*)$ if one of the following conditions holds: (a) $\frac{eaK}{m} > 1$ and $H(\eta) < 0$; (b) $\frac{eaK}{m} < 1$, $b < \frac{a^2}{r}$, $H'(\gamma_2) < 0$ and $H(\eta) < 0$.

Next, we investigate the stability of equilibria of model (3), and the expression of Jacobin matrix is

$$J = \begin{bmatrix} r(1-\frac{2}{K}N) - (a+bP)P & -N(a+2bP) \\ e\frac{P}{\alpha+P}(a+bP)P & -m+eN\left[\frac{\alpha}{(\alpha+P)^2}(a+bP)P + \frac{P}{\alpha+P}(a+2bP)\right] \end{bmatrix}.$$

It is easy to obtain that the Jacobin matrix at E_0 has two eigenvalues $\lambda_1 = r$, $\lambda_2 = -m$. Thus, the boundary equilibrium E_0 is unstable. Similarly, the Jacobin matrix at E_K has two eigenvalues $\lambda_1 = -r$, $\lambda_2 = eaK - m$, and we know that the boundary equilibrium E_K is always locally stable if eaK < m and unstable of eaK > m.

Let $E_{\#}(N_{\#}, P_{\#})$ be any positive equilibrium $E_1^*(N_1^*, P_1^*)$ or $E_2^*(N_2^*, P_2^*)$ where $P_1^* < P_2^*$. After extensive algebraic calculations, the corresponding characteristic equation at $E_{\#}$ is

$$f(\lambda) = \lambda^2 + A_1(N_{\#}, P_{\#})\lambda + A_2(N_{\#}, P_{\#}) = 0, \tag{10}$$

where

$$A_1(E_\#) = \frac{r}{K} N_\# - e \frac{N_\# P_\#}{\alpha + P_\#} \left[b P_\# + \frac{\alpha}{\alpha + P_\#} (a + b P_\#) \right]$$

$$A_2(E_\#) = -\frac{mr}{K} P_\# F'(P_\#).$$

Let $\lambda_1(E_\#)$, $\lambda_2(E_\#)$ be the roots of (10), and assume that $\Re \lambda_1(E_\#) \leq \Re \lambda_2(E_\#)$. Then by using the same arguments as the proof in Appendix B, we summarize the following results: The positive equilibrium E_1^* is a saddle when it exists; The positive equilibrium E_2^* is locally asymptotically stable if $\frac{r}{K} > eb \frac{P_2^{*2}}{\alpha + P_2^*} + e \frac{\alpha P_2^*}{(\alpha + P_2^*)^2} (a + bP_2^*)$, and it is unstable if $\frac{r}{K} < eb \frac{P_2^{*2}}{\alpha + P_2^*} + e \frac{\alpha P_2^*}{(\alpha + P_2^*)^2} (a + bP_2^*)$.

Appendix E. Proof of Theorem 5

Evaluating the Jacobin matrix of model (2.4) at E_0 gives three eigenvalues $\lambda_1 = r$, $\lambda_2 = -m$, $\lambda_3 = -\mu$. Thus, the boundary equilibrium E_0 of model (4) is unstable. Similarly, the eigenvalues of Jacobin matrix at E_K are $\lambda_1 = -r$, $\lambda_2 = -m$, $\lambda_3 = -\mu - m$ i.e., the boundary equilibrium E_K is locally asymptotically stable.

Let $E_S(N_S, S_S, 0)$ be E_1^S or E_2^S . The Jacobin of model (4) at E_S is

$$J(E_S) = \begin{bmatrix} A_{11} & A_{12} \\ 0 & \beta S_S - \mu \end{bmatrix},$$

where

$$A_{11} = \begin{bmatrix} -\frac{r}{K}N_S & -N_S(a+2bS_S) \\ e\frac{S_S}{\alpha+S_S}(a+bS_S)S_S & eN_S\frac{S_S}{\alpha+S_S}\left[\frac{S_S}{\alpha+S_S}(a+bS_S)+bS_S\right] \end{bmatrix},$$

$$A_{12} = \begin{bmatrix} -N_S(a+2bS_S) \\ -\beta S_S + eN_S \frac{S_S}{\alpha+S_S} \left[\frac{S_S}{\alpha+S_S} (a+bS_S) + bS_S \right] \end{bmatrix}.$$

According to Theorem 4, the boundary equilibrium E_1^S of model (4) is always a saddle, and the boundary equilibrium E_2^S of model (4) is locally asymptotically stable if it is locally asymptotically stable on the N-S coordinate plane, i.e., $\frac{r}{K} > eb \frac{(S_2^S)^2}{\alpha + S_2^S} + e \frac{\alpha S_{12}}{(\alpha + S_2^S)^2} (a + bS_2^S)$, and $S_2^S < \frac{\mu}{\beta}$. By using the same arguments, it can be concluded that the boundary equilibrium E_1^I is a saddle, and the boundary equilibrium E_2^I is locally asymptotically stable if $\frac{r}{K} > eb \frac{(l_2^I)^2}{\alpha + l_2^I} + e \frac{\alpha l_2^I}{(\alpha + l_2^I)^2} (a + bl_2^I)$ and $l_2^I > \frac{\mu}{\beta}$.

Define $h = b \frac{\frac{\mu}{\beta}}{\alpha + \frac{\mu}{\beta}} + \frac{\alpha}{\left(\alpha + \frac{\mu}{\beta}\right)^2} \left(a + b \frac{\mu}{\beta}\right)$, and the Jacobin matrix of model (4) at E_* is

$$J(E_*) = \begin{bmatrix} -\frac{r}{R}N_* & -(a+2b\frac{\mu}{\beta})N_* & -(a+2b\frac{\mu}{\beta})N_* \\ e\frac{\frac{\mu}{\beta}}{\alpha+\frac{\mu}{\beta}}(a+b\frac{\mu}{\beta})S_* & ehN_*S_* & -\beta S_* + ehN_*S_* \\ e\frac{\frac{\mu}{\beta}}{\alpha+\frac{\mu}{\beta}}(a+b\frac{\mu}{\beta})I_* & \beta I_* + ehN_*I_* & ehN_*I_* \end{bmatrix}.$$

After extensive algebraic calculations, the characteristic equation is

$$f(\lambda) = \lambda^3 + a_2(E_*)\lambda^2 + a_1(E_*)\lambda + a_0(E_*) = 0,$$
(11)

where

$$\begin{split} a_2(E_*) &= \frac{r}{K} N_* - eh \frac{\mu}{\beta} N_*, \\ a_1(E_*) &= \beta^2 S_* I_* + (a + 2b \frac{\mu}{\beta}) (m \frac{\mu}{\beta} + \mu I_*) - \frac{erh}{K} \frac{\mu}{\beta} N_*^2, \\ a_0(E_*) &= \frac{\beta^2 r}{K} N_* S_* I_*. \end{split}$$

It then follows from the expression of $a_0(E_*)$ that $a_0(E_*) > 0$. Let $\lambda_1(E_*)$, $\lambda_2(E_*)$ and $\lambda_3(E_*)$ be the roots of (11). We assume that $\Re \lambda_1(E_*) < \Re \lambda_2(E_*) \le \Re \lambda_3(E_*)$. From the relations between the roots and the polynomial coefficients, we have that

$$a_2(E_*) = -(\lambda_1(E_*) + \lambda_2(E_*) + \lambda_3(E_*)),$$

$$a_0(E_*) = -\lambda_1(E_*)\lambda_2(E_*)\lambda_3(E_*) > 0.$$

This indicates that either $\Re\lambda_1(E_*) < 0 \le \Re\lambda_2(E_*) \le \Re\lambda_3(E_*)$ or $\Re\lambda_1(E_*) < \Re\lambda_2(E_*) \le \Re\lambda_3(E_*) \le 0$. Therefore, if $a_1(E_*)a_2(E_*) > a_0(E_*)$ and $a_1(E_*) > 0$, $a_2(E_*) > 0$, according to Routh-Hurwitz conditions, the roots of (11) are $\Re\lambda_i(E_*) < 0$, i=1,2,3. By using the Hartman-Grobman theorem, we have $\dim W^S(E_*) = 3$, i.e., the positive equilibrium $E_*(N_*,S_*,I_*)$ is locally asymptotically stable. If $a_1(E_*)a_2(E_*) > a_0(E_*)$ and $a_1(E_*) < 0$, $a_2(E_*) < 0$, one can verify that $\Re\lambda_1(E_*) < 0 < \Re\lambda_2(E_*) \le \Re\lambda_3(E_*)$, and we have $\dim W^S(E_*) = 1$, $\dim W^U(E_*) = 2$ by using the Hartman-Grobman theorem, i.e., the positive equilibrium $E_*(N_*,S_*,I_*)$ is unstable. If $a_1(E_*)a_2(E_*) < a_0(E_*)$, one can verify that $\Re\lambda_1(E_*) < 0 < \Re\lambda_2(E_*) < \Re\lambda_3(E_*)$. By using the Hartman-Grobman theorem, we have $\dim W^S(E_*) = 1$, $\dim W^U(E_*) = 2$, i.e., the positive equilibrium $E_*(N_*,S_*,I_*)$ is unstable. If $a_1(E_*)a_2(E_*) = a_0(E_*)$ and $a_1(E_*) < 0$, $a_2(E_*) < 0$, we have $\lambda_1(E_*) = -a_2(E_*)$, $\lambda_{2,3}(E_*) = \pm \sqrt{-a_1(E_*)}$. It follows from Hartman-Grobman theorem that $\dim W^S(E_*) = 1$, $\dim W^U(E_*) = 2$. If $a_1(E_*)a_2(E_*) = a_0(E_*)$ and $a_1(E_*) > 0$, $a_2(E_*) > 0$, then the roots are $\lambda_1(E_*) = -a_2(E_*)$, $\lambda_{2,3}(E_*) = \pm i\sqrt{a_1(E_*)}$. It indicates that $\dim W^S(E_*) = 1$, $\dim W^C(E_*) = 2$.

References

- [1] K.F. Smith, D.F. Sax, K.D. Lafferty, Evidence for the role of infectious disease in species extinction and endangerment, Conserv. Biol. 20 (5) (2006)
- [2] W.H. Organization, et al., Mortality and global health estimates, World Health Organization: Geneva, Switzerland, 2013.
- [3] P.T. Johnson, J.C. De Roode, A. Fenton, Why infectious disease research needs community ecology, Science 349 (6252) (2015) 1259504.
- [4] F. Keesing, L.K. Belden, P. Daszak, A. Dobson, C.D. Harvell, R.D. Holt, P. Hudson, A. Jolles, K.E. Jones, C.E. Mitchell, et al., Impacts of biodiversity on the emergence and transmission of infectious diseases, Nature 468 (7324) (2010) 647–652.
- [5] M.E. Scott, The impact of infection and disease on animal populations: implications for conservation biology, Conserv. Biol. 2 (1) (1988) 40–56.
- [6] J. Chattopadhyay, N. Bairagi, Pelicans at risk in Salton sea an eco-epidemiological model. Ecol. Model, 136 (2-3) (2001) 103-112.
- [7] Y. Xiao, L. Chen, Analysis of a three species eco-epidemiological model, J. Math. Anal. Appl. 258 (2) (2001) 733-754.
- [8] M. Otero, H.G. Solari, Stochastic eco-epidemiological model of dengue disease transmission by aedes aegypti mosquito, Math. Biosci. 223 (1) (2010) 32-46
- [9] B. Mukhopadhyay, R. Bhattacharyya, Role of predator switching in an eco-epidemiological model with disease in the prey, Ecol. Model. 220 (7) (2009) 931–939.
- [10] T. Feng, D. Charbonneau, Z. Qiu, Y. Kang, Dynamics of task allocation in social insect colonies: scaling effects of colony size versus work activities, J. Math. Biol. 82 (5) (2021) 1–53.
- Math. Biol. 82 (5) (2021) 1-53.
 [11] R.M. Anderson, R.M. May, The invasion, persistence and spread of infectious diseases within animal and plant communities, Philos. Trans. R. Soc. Lond.
- B Biol. Sci. 314 (1167) (1986) 533–570. [12] S.K. Sasmal, J. Chattopadhyay, An eco-epidemiological system with infected prey and predator subject to the weak Allee effect, Math. Biosci. 246 (2)
- (2013) 260–271.
 [13] Y. Kang, S.K. Sasmal, A.R. Bhowmick, J. Chattopadhyay, Dynamics of a predator-prey system with prey subject to Allee effects and disease, Math. Biosci.
- Eng. 11 (4) (2014) 877–918.

 [14] M. Su, C. Hui, Y. Zhang, Z. Li, Spatiotemporal dynamics of the epidemic transmission in a predator-prey system, Bull. Math. Biol. 70 (8) (2008) 2195.
- [15] N.M. Oliveira, F.M. Hilker, Modelling disease introduction as biological control of invasive predators to preserve endangered prey, Bull. Math. Biol. 72 (2) (2010) 444–468.
- [16] A.M. Bate, F.M. Hilker, Complex dynamics in an eco-epidemiological model, Bull. Math. Biol. 75 (11) (2013) 2059-2078.
- [17] L. Berec, E. Angulo, F. Courchamp, Multiple Allee effects and population management, Trends Ecol. Evol. 22 (4) (2007) 185-191.
- [18] L. Berec, D.S. Boukal, M. Berec, Linking the Allee effect, sexual reproduction, and temperature-dependent sex determination via spatial dynamics, Am. Nat. 157 (2) (2001) 217–230.
- [19] F. Courchamp, D.W. Macdonald, Crucial importance of pack size in the african wild dog Lycaon Pictus, in: Animal Conservation forum, 4, Cambridge University Press, 2001, pp. 169–174.
- [20] J. Gascoigne, R.N. Lipcius, Allee effects in marine systems, Mar. Ecol. Prog. Ser. 269 (2004) 49-59.
- [21] A. Bourbeau-Lemieux, M. Festa-Bianchet, J.-M. Gaillard, F. Pelletier, Predator-driven component Allee effects in a wild ungulate, Ecol. Lett. 14 (4) (2011) 358–363.
- [22] A.J. Terry, Predator-prey models with component Allee effect for predator reproduction, J. Math. Biol. 71 (6-7) (2015) 1325-1352.
- [23] P. Aguirre, E. González-Olivares, E. Sáez, Three limit cycles in a Leslie–Gower predator-prey model with additive Allee effect, SIAM J. Appl. Math. 69 (5) (2009) 1244–1262.
- [24] P. Aguirre, E. González-Olivares, E. Sáez, Two limit cycles in a Leslie–Gower predator–prey model with additive Allee effect, Nonlinear Anal. Real World Appl. 10 (3) (2009) 1401–1416.

- [25] D.W. Macdonald, The ecology of carnivore social behaviour, Nature 301 (5899) (1983) 379-384.
- [26] D.A. Clayton, Socially facilitated behavior, Q. Rev. Biol. 53 (4) (1978) 373-392.
- [27] R. Bshary, A. Hohner, K. Ait-el Djoudi, H. Fricke, Interspecific communicative and coordinated hunting between groupers and giant moray eels in the red sea, PLoS Biol. 4 (12) (2006).
- [28] F.M. Hilker, M. Paliga, E. Venturino, Diseased social predators, Bull. Math. Biol. 79 (10) (2017) 2175-2196.
- [29] A.M. Bate, F.M. Hilker, Disease in group-defending prey can benefit predators, Theor. Ecol. 7 (1) (2014) 87–100.
- [30] M.T. Alves, F.M. Hilker, Hunting cooperation and Allee effects in predators, J. Theor. Biol. 419 (2017) 13–22.
- [31] D. Scheel, C. Packer, Group hunting behaviour of lions: a search for cooperation, Anim. Behav. 41 (4) (1991) 697-709.
- [32] S. Creel, N.M. Creel, Communal hunting and pack size in african wild dogs, Lycaon Pictus, Anim. Behav. 50 (5) (1995) 1325-1339.
- [33] P.A. Schmidt, L.D. Mech, Wolf pack size and food acquisition, Am. Nat. 150 (4) (1997) 513-517.
- [34] D.P. Hector, Cooperative hunting and its relationship to foraging success and prey size in an avian predator, Ethology 73 (3) (1986) 247-257.
- [35] M.W. Moffett, Foraging dynamics in the group-hunting myrmicine ant, pheidologeton diversus, J. Insect Behav. 1 (3) (1988) 309-331.
- [36] C. Cosner, D.L. DeAngelis, J.S. Ault, D.B. Olson, Effects of spatial grouping on the functional response of predators, Theor. Popul. Biol. 56 (1) (1999) 65–75.
- [37] L. Berec, Impacts of foraging facilitation among predators on predator-prey dynamics, Bull. Math. Biol. 72 (1) (2010) 94-121.
- [38] L. Avilés, P. Tufino, Colony size and individual fitness in the social spider anelosimus eximius, Am. Nat. 152 (3) (1998) 403-418.
- [39] E. Francomano, F.M. Hilker, M. Paliaga, E. Venturino, Separatrix reconstruction to identify tipping points in an eco-epidemiological model, Appl. Math. Comput. 318 (2018) 80–91.
- [40] J.W. McNutt, Sex-biased dispersal in african wild dogs, Lycaon Pictus, Anim. Behav. 52 (6) (1996) 1067-1077.
- [41] M.W. Coulter, The wolf: the ecology and behavior of an endangered species, 1971.
- [42] J.L. Stenglein, T.R. Van Deelen, Demographic and component Allee effects in southern lake superior gray wolves, PloS One 11 (3) (2016).
- [43] M. McCarthy, The allee effect, finding mates and theoretical models, Ecol. Model. 103 (1) (1997) 99-102.
- [44] J. Wang, J. Shi, J. Wei, Predator-prey system with strong Allee effect in prey, J. Math. Biol. 62 (3) (2011) 291-331.
- [45] S.V. Petrovskii, A.Y. Morozov, E. Venturino, Allee effect makes possible patchy invasion in a predator-prey system, Ecol. Lett. 5 (3) (2002) 345-352.
- [46] A. Morozov, S. Petrovskii, B.L. Li, Bifurcations and chaos in a predator-prey system with the Allee effect, Proc. R. Soc. Lond. Ser. B Biol. Sci.s 271 (1546) (2004) 1407–1414.
- [47] J. Wang, J. Shi, J. Wei, Dynamics and pattern formation in a diffusive predator–prey system with strong Allee effect in prey, J. Differ. Equ. 251 (4-5) (2011) 1276–1304.